Available online at www.sciencedirect.com
SCIENCE DIRECT
Polymer 46 (2005) 8662–8681
polymer
www.elsevier.com/locate/polymer

Enthalpic and entropic origins of nucleation barriers during polymer crystallization: the Hoffman–Lauritzen theory and beyond

Stephen Z.D. Cheng[a,*], Bernard Lotz[b]

[a]*Maurice Morton Institute and Department of Polymer Science, The University of Akron, Akron, OH 44325-3909, USA*
[b]*Institute Charles Sadron, 6 Rue Boussingault, Strasbourg 67083, France*

Received 8 November 2004; received in revised form 15 February 2005; accepted 11 March 2005
Available online 29 June 2005

Abstract

In the search for a greater understanding of polymer crystallization, numerous experimental observations with regards to microscopic structures and macroscopic properties have been reported in the past half-century. There are generally two types of experimental results to provide information about the mechanisms of polymer crystal growth, i.e. molecular dynamic/scattering and structural/morphological. Since we cannot follow the trajectory of individual chain molecules when they undergo the transition from liquid to solid state during the crystallization process, structural/morphological analysis of polymer crystals reveal information recorded during this process. Namely, the final structure and morphology of polymer crystals have atomic, stem and global chain conformation information embedded in them during crystallization which provides evidence which can be used to deduce molecular aspects of the polymer crystallization process. It is commonly understood that polymer crystallization, from the thermodynamic perspective, is a first-order transition involving the relaxation of a metastable undercooled melt towards the equilibrium state which is rarely reached in polymer crystals. This process is controlled by a free energy barrier. A molecular model is required to describe the landscape of the free energy barriers and to provide an analytical explanation concerning and predictions about polymer crystallization. The Hoffman–Lauritzen (HL) theory, which was put forward more than 40 years ago, was one of the first analytical theories to illustrate how polymers crystallize. Since then, modifications to the HL theory and suggestions for new approaches have been reported, but the core physical picture of the HL theory has largely remained intact. This article consists of four major parts: (1) we will compare the crystallization of small molecules and long chain molecules, and the relationship between crystallization and crystal habits. The diversity of crystalline structures and morphologies of semi-crystalline polymers must be taken into account when studying the crystallization mechanism of polymers (2) this article also serves as a brief review of the HL theory and its importance in our understanding of polymer crystallization (3) we have tried to answer the question: what is the nucleation barrier? Specifically, we will illustrate that the nucleation barrier in polymer crystallization consists of both enthalpic and entropic components as deduced from experimental results. This barrier, from our perspective, consists of selection processes taking place in different length- and time-scales (4) finally, there is a brief discussion on what issues remain, in particular, in the areas of undercooled liquid structures and the initial stages of crystallization.

Keywords: Crystal structure; Crystal growth; Crystallization

1. General introduction to polymer crystal growth

The crystallization of small molecules from vapor, solution, or the melt is described by both three-dimensional (3D) homogeneous (primary) nucleation and crystal growth (secondary nucleation) on an existing crystal surface. As early as the 18th century, it was recognized that these processes do not necessarily take place at equilibrium [1]. The concept of primary nucleation is based on an assumption that thermal fluctuations in an undercooled phase can overcome the nucleation barrier caused by the surface free energy of small crystals. At a constant volume and energy, the probability that a nucleus of a given size exists is a function of the entropic change based on the Boltzmann's law, which is proportional to $\exp(\Delta S/k)$ (where k is the Boltzmann constant). At constant pressure and temperature, the probability that a nucleus of a given size

* Corresponding author. Tel.: +1 330 972 6931; fax: +1 330 972 8626.
E-mail addresses: scheng@uakron.edu (S.Z.D. Cheng), lotz@ics.u-strasbg.fr (B. Lotz).

0032-3861/$ - see front matter © 2005 Elsevier Ltd. All rights reserved.
doi:10.1016/j.polymer.2005.03.125

exists is proportional to $\exp[-\Delta G/(kT)]$. Turnbull and Fisher derived an equation for the rate of nucleation (i) based on the small crystal model, and this equation is dominated by two opposing factors: the free energy of the nucleation barrier (ΔG) and the free energy of activation (ΔG_η) [2]:

$$i = \left(\frac{NkT}{h}\right)\exp\left[-\frac{(\Delta G + \Delta G_\eta)}{kT}\right] \quad (1)$$

where h is the Planck constant, and N, the number of uncrystallized elements that act as single units which participate in the nucleation process. It was also found that Eq. (1) could also represent, in a general thermodynamic form, heterogeneous (secondary) nucleation processes. In this case, molecules undergo a nucleation-controlled process on an atomically smooth surface, and the nucleation rate exhibits an exponential dependence with respect to both the free energies of the nucleation barrier and the activation. For single crystal growth in a nucleation-controlled process, well-defined macroscopic facets in single crystal habits are expected to form sectors, which are determined by the slowest crystal growth planes during the growth. This nucleation process is known as lateral growth and it describes molecules that crystallize on an existing smooth crystal surface in either dilute or condensed states.

A fundamentally different growth model, the so-called continuous growth model [3], implies that the crystal grows on an atomically rough surface, such that every impingement site is a potential growth site. As a result, surface diffusion and the actual surface morphology can be ignored. This leads to a linear relationship between the growth rate and the undercooling ($\Delta T = T_m - T_c$, where T_m is equilibrium melting temperature and T_c is crystallization temperature) at low ΔTs. At high ΔTs, the growth rate exhibits an exponential dependence on the free energy of activation. The single crystal habits are, in this case, dominant by concentration and/or temperature gradients during crystallization in dilute and condensed states. With this growth behavior, the shape of a single crystal is a true replica of the concentration and/or temperature profiles, but cannot produce faceted crystal habits from crystallographic growth planes. As a result, curved crystals are generated. Note that the absence of macroscopic facets in curved single crystal habits does not necessarily imply that the continuous crystal growth mechanism was dominate. The critical issue between these two different growth models is the roughness criteria of the crystal growth front. Namely, at what degree of the surface roughness does the crystal growth behavior change from one mechanism to another? Although this is clearly defined in the crystallization of small molecules, a quantitative assessment in polymer crystallization has yet to be achieved.

Even before the acceptance of polymers as chemically connected long chain molecules, wide angle X-ray diffraction (WAXD) experiments on some natural and synthetic polymers had revealed structural features. The Bragg diffractions of those polymers were broad and diffuse compared to those of well-developed small molecule single crystals, and these features were attributed to small crystal sizes as well as the existence of defects based on diffraction theory. These crystals were described originally as fringed micelles [4]. In the early to mid 1950s, polymer single crystals with crystallographically defined, facetted shapes were observed in dilute solutions with optical microscopy and transmission electron microscopy (TEM) [5–7], and later, via TEM experiments in the melt [8,9] implying a nucleation controlled process. Fig. 1 shows a TEM bright-field image of polyethylene (PE) single crystals grown in dilute solution. Electron diffraction (ED) provided direct experimental observations to enable interpretation of how the long chain molecules crystallize into the lamellar form. The concept of chain folding was proposed at that time by Keller [6], the origin of which can be traced back to 1938 [10]. This concept as a whole is widely accepted today despite controversies about some details regarding how the chains fold. At the same time, the observation of polymeric spherulites in the melt [11–14], and dendrites [15–18] in solution were also reported, which are analogous to crystal aggregates in small molecules. These experimental observations implied that the lamellar single crystals are the basic underlying building blocks of these polymer crystal aggregates.

It was also found that polymers, even chemically uniform homo-polymers, have extreme difficulty in crystallizing fully. There is no single local barrier that is responsible for the halting of growth. It is rather a range of essentially kinetic factors, rooted in the long chain nature of polymers, which hamper the polymers from becoming fully incorporated into the crystals. So to more precisely describe crystalline polymer materials, the concept of crystallinity, which is the ratio of crystalline volume with respect to overall (crystalline plus amorphous) volume, was developed.

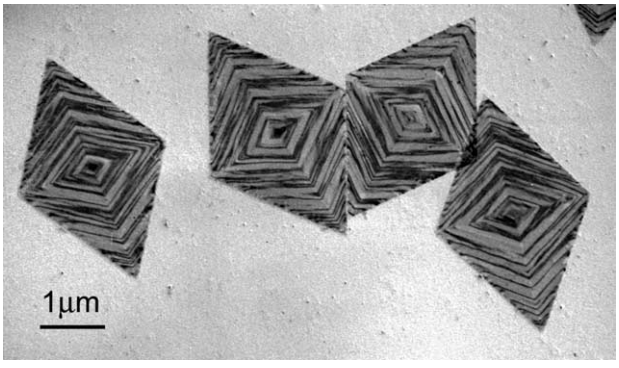

Fig. 1. Polyethylene single crystals grown in dilute solution. This is a bright field TEM micrograph of a so-called corrugated crystal. The dark stripes normal to the growth faces are due to Bragg contrast (the corresponding areas scatter electrons that do not therefore contribute to the image) (Courtesy of Prof J.C. Wittmann).

With a large number of lamellar single crystals observed and their crystal unit cell dimensions and symmetry groups determined, it was found that polymer single crystals possess a variety of habits ranging from elongated ribbon-like (kinetically anisotropic) to square or hexagonal shaped (kinetically isotropic) single crystals formed both from the melt and solution [19–24]. The formation of the anisotropic single crystal morphology implies that the growth rate along one specific crystallographic direction is faster than along others. Therefore, the nucleation barrier for polymers to crystallization at growth fronts corresponding to specific crystallographic directions is different. The isotropic single crystal habit is generated by the identical growth rates along all the growth front normals, since they actually belong to the same set of {*hkl*} planes, and thus, possess a single nucleation barrier. Generally speaking, a unit cell with lower rotational symmetry with the *c*-axis generates an anisotropic single crystal habit, while a unit cell with higher rotational symmetry generates an isotropic single crystal habit [21,24]. Examples include single crystals of PE in the orthorhombic form grown in solution [25–28] and the melt [29–33], isotactic polypropylene (it-PP) in the monoclinic α-form grown from solution [34–36], syndiotactic polypropylene (st-PP) in the high-temperature orthorhombic form (as shown in Fig. 2(a)) [37–43], poly(vinylidiene fluoride) (PVDF) in the orthorhombic α-form in the melt [44,45] and others. All of them possess unit cells having 2_1 rotational symmetry with the *c*-axis, and they thus exhibit elongated single crystal habits. On the other hand, PE single crystals in the high-pressure hexagonal form (as shown in Fig. 2(b)) [46,47], poly(oxymethylene) (POM) in the trigonal form in solution [48,49], isotactic polystyrene (it-PS) in the trigonal form grown in the melt [50,51], poly-4-methyl-1-pentene (PMP) in the tetragonal form in solution [52–56] and others possess higher rotational symmetry with the *c*-axis in their crystal unit cells (3_1, 4_1 or 6_1) and exhibit polygonal lamellar habits.

The correlation between unit cell symmetry and crystal habit begs the following question; what occurs when a polymorphous crystalline polymer transforms from a crystal structure with a higher lattice symmetry to another form with a lower lattice symmetry? The answer depends on whether the transformation takes place in the form of a solid–solid transition or a solid–liquid–solid transition. A solid–solid transformation occurs when the hexagonal phase of PE is grown at an elevated pressure and transforms to the orthorhombic PE crystal form when the pressure is lowered. This can give rise to twinned symmetries having three equivalent orientations 120° apart from each other [47] (Fig. 2(b)). However, PE spherulites at atmospheric pressure always grow with the *b*-axis of the orthorhombic structure in the radial direction, and no twin symmetry can be found [11–14]. Therefore, the morphological memory of the single crystal with high unit-cell symmetry is retained in this solid–solid transition. On the other hand in a solid–liquid–solid transformation, memory of the original single crystal morphology is lost in the transition to the liquid state. Only the latest structural symmetry determines the newly formed single crystal habit [57].

By combining the significance of the chain folded lamellar crystal and its aggregates on different length scales with measured crystal growth rates, kinetic descriptions bridging macroscopic crystal characteristics to microscopic molecular behaviors during crystallization can be made. One of the first and by far the most resilient of these theories is the Hoffman–Lauritzen (HL) theory. It provides a simple, yet incisive, mean-field picture of how polymer crystallization proceeds. Through subsequent modifications, this theory has been able to accommodate major features in the crystal growth of PE and can be generalized for use in other polymer systems. In the following parts of this article, we will present the physical core of the HL theory and discuss how it has been modified to accommodate new experimental findings. We will then further elucidate a concept critical to HL theory, the nucleation barrier. Based on structural and morphological analysis, we will present evidence to show which factors contribute to the nucleation barrier of semi-crystalline polymers. Finally, we will go into areas where we think there are opportunities for new and important efforts to be made.

2. Brief description of the Hoffman–Lauritzen theory

The crystallization process converts chain molecules that are in 3D random coil conformations to chain folded lamellar crystals. The specific trajectory of an individual chain molecule during crystallization may be very different from others. Yet, we lack a technique to monitor each chain molecule to 'see' how it crystallizes. An analytical theory always takes a 'mean-field' approach by simplifying the individual trajectories into an average form. Therefore, the analytical theory sacrifices these molecular details.

The first analytical theories were put forth more than 40 years ago by Hoffman and Lauritzen [58–61] and Frank and Tosi [62]. They utilized a lateral growth, surface-nucleation controlled process to describe the growth rates of polymer lamellar crystals. The molecular picture of this surface nucleation is clear. An existing crystal with a defined atomically smooth crystallographic surface provides a growth front. Chain molecules deposit onto the growth plane and start to crystallize onto the lattice one stem at a time to form lamellae. The crystal growth rate perpendicular to the growth front is linear at a constant T_c. This kinetic model contains four parameters to describe the nucleation process: the surface nucleation rate, *i*; the growth rate parallel to the growth plane that covers the growth front after the surface nucleation which is called the lateral covering rate, *g*; the width of the growth front (the substrate length) which the nucleation and growth covers, *L*; and the growth rate perpendicular to the growth plane, *G*. The HL theory predicts three growth regimes which are shown in

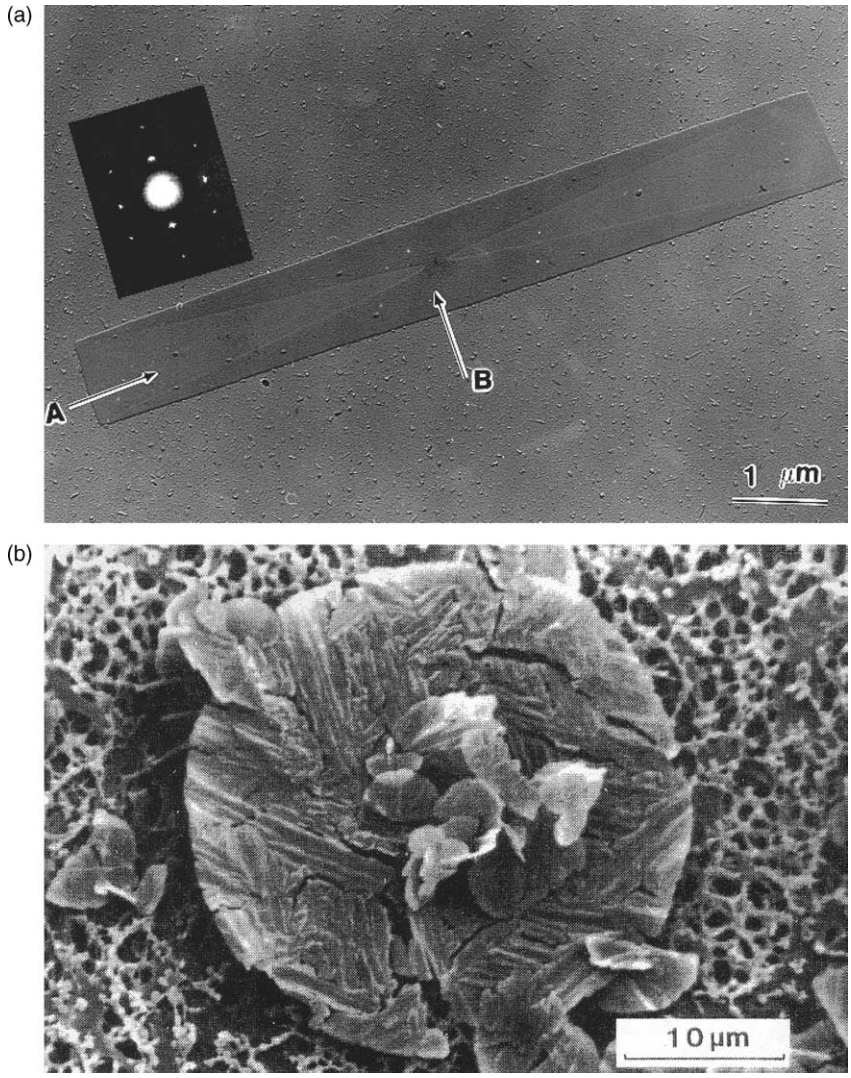

Fig. 2. Lamellar single crystals of polymers grown from melt and solution (a) st-PP lamellar single crystal grown in the melt. Reprinted from [41] with permission (b) PE extended chain single crystal grown in the melt at elevated pressure. Reprinted from [47] with permission.

Fig. 3(a)–(c). At low ΔTs, regime I takes place when the growth from a single nucleus covers the entire growth plane L as shown in Fig. 3(a). The physical picture of this process is that given an atomically smooth growth front, the rate controlling surface nucleation occurs first, the rest of the growth front is quickly covered by lateral growth to generate a new atomically smooth growth front, which then, waits for the formation of the next nucleus on the new front. The analytical expression for the growth rate in regime I is given by [58–63]:

$$G_{\mathrm{I}} = ib_0L \tag{2}$$

Here b_0 is the thickness of the molecular layer crystallized on the substrate, and L is the substrate length which is covered by one surface nucleus under a condition that $g/L \ll iL$ [64].

With increasing ΔT, Fig. 3(b) illustrates the physical picture of regime II growth. It is evident that on the substrate of width L, more than one nucleus is formed. Therefore, the growth rates are now associated with the parameters i and g. The critical factor in this regime is the niche separation between two neighboring nuclei. At the higher end of T_c in regime II, the niche separation is large. As the nucleation rate increases with increasing ΔT, the niche separation is continuously reduced. The analytical expression of the growth rate in regime II is given by:

$$G_{\mathrm{II}} = (ib_0g)^{1/2} \tag{3}$$

and this is independent of L [63,65,66]. Frank also derived Eq. (3) using a differential equation with defined boundary conditions [64]. This equation possesses analytical solutions with moving boundary conditions that predict different morphological shapes of the PE single crystals from the lozenge to the lenticular shape by Mansfield and Toda [67,68]. An analysis of the morphological shape change from

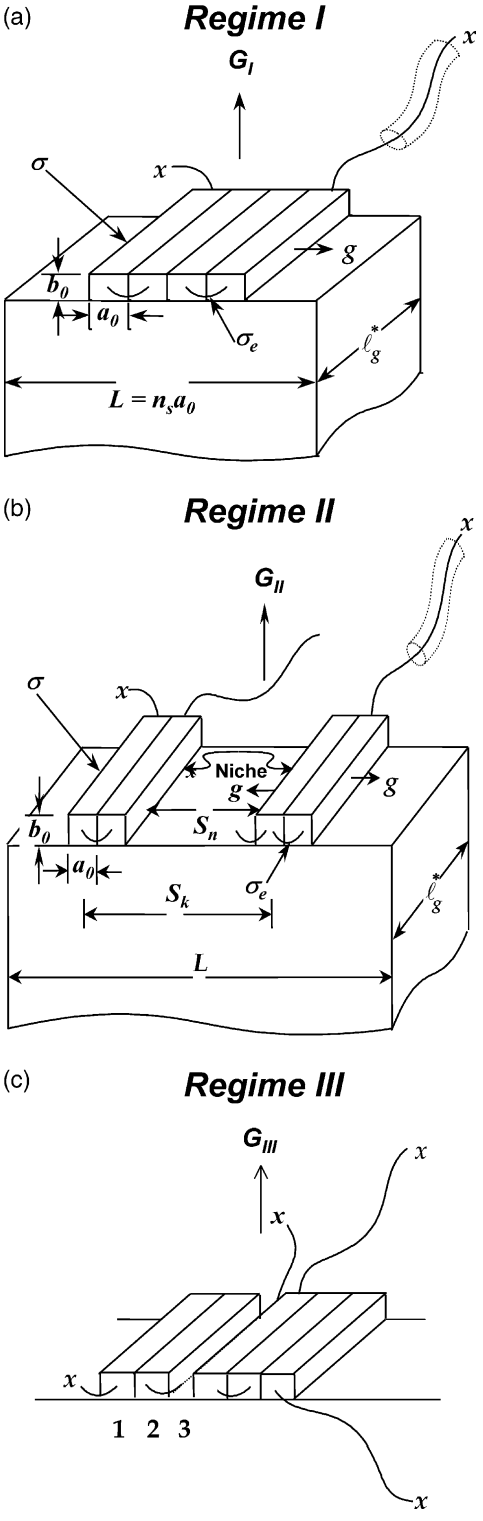

Fig. 3. Schematic drawings of how polymer crystal growth takes place in three regimes: (a) regime I; (b) regime II; and (c) regime III. Reprinted from [63,70] with permissions. The 'x' represents chain ends.

the lozenge to the truncated lozenge habits was earlier reported by Passaglia and Khoury [69].

Upon further decreasing the T_c, one passes into the lower T_c end of regime II resulting in changes in the crystal growth, and then, one enters regime III as shown in Fig. 3(c). The niche separation distance reaches the same order of magnitude as the stem width a_0. Therefore, the lateral covering rate g is not a dominant factor, so the analytical expression for the growth rate returns back to:

$$G_{III} = ib_0L' \tag{4}$$

Here L' is the width between two neighboring niches, which is about 1–3 stem widths [70,71].

Since the surface-nucleation rate i always takes the Turnbull and Fisher form (Eq. (1)) [2], the linear growth rate G is always in some type of exponential relationship with the free energies of the nucleation barrier and activation. Since the free energy of activation at high T_c values is almost constant, significant attention has been focused on the free energy of the nucleation barrier. Based on the original HL theory, the nucleation barrier to polymer crystal growth is caused by the lateral and folded surface free energies ($A\gamma$ and $B\gamma_e$, where γ and γ_e are lateral and fold surface free energy densities, and A and B, lateral and fold surface areas) overwhelming the bulk free energy of crystals (Vg_f, where g_f is bulk free energy density, and V, the volume of the crystal) when the crystal is small. A detailed analytical construction of this nucleation barrier depends on how the chain molecules place themselves into the crystalline lattice. The HL theory assumes as the averaging step in its 'mean-field' approach that the stems attach onto the crystal growth front one at a time. Other approaches use a few segments at a time as suggested by Point [72,73], or a few stems at a time as proposed by Phillips [74,75]. These differences in detail may change the outcome of those four structural parameters during the crystal growth, but the overall exponential dependence of the growth rate G with respect to the nucleation barrier is not altered. Among these four parameters, in most cases, only the linear growth rate G can be experimentally measured. In the specific case of measuring the single crystal growth of PE, the lateral covering rate g can also be deduced [33]. Other parameters can be understood indirectly using supplemental experimental methods such as the coherence length measured via the WAXD method which corresponds to the substrate length L crystallized in the melt [76] (this may not work in the case of solution crystallization).

Since the HL theory was originally proposed, it has undergone continuous improvements and modifications to accommodate new experimental findings and theoretical understandings. This is a simple reflection of the flexibility of this theory and the ability to manipulate structural parameters based on improved understandings of their physical significance. The first modification was in response to the so-called 'δl catastrophy' [58,59,77,78]. Based on the first version of the HL theory, one expects that the lamellar thickness goes to infinity at $\Delta g_f = 2\gamma/a_0$. This can be overcome by introducing a parameter Ψ into the HL theory that apportions a fraction of the free energy of

crystallization to the free energy associated with stem attachment, while the remainder was released during subsequent rearrangement of the attached stem. The second modification dealt with the substrate length, L, which initially was speculated to be on the order of micrometers. However, later experimental results based on an outstanding experiment designed to measure the crystal growth rate of PE single crystals in solution with a well-controlled temperature-jumping technique showed that this value should be much smaller [79]. This is based on the experimental observation that PE single crystal growth rates exhibit a linear behavior down to at least the micrometer resolution of the experiment, while the HL theory predicts that the crystal growth rate has to increase as long as the crystal lateral size is smaller than L [79]. This result implies that the substrate length L in the LH theory must be smaller than one micrometer. Currently, it is thought that these values should be several tens of nanometers which corresponds to the crystallite size measured via WAXD experiments [76,77,80,81]. The third modification was to account for the growth rate minimum found in n-alkanes in both the melt and solution around the vicinity of T_cs where the once-folded integral chain [IF($n=1$)] crystals convert to extended chain [IF($n=0$)] crystals [82]. The introduction of an entropic component to the lateral surface free energy γ which is attributed to a transient layer of 'kinetic ciliation' allows the HL theory to reproduce the experimentally observed rate minimum [83]. Furthermore, the introduction of the C_∞ term (the characteristic ratio of the polymers in the melt) into the presentation of the lateral surface free energy γ was also suggested [84,85]. The fourth modification was meant to explain how the HL theory can be applied to curved growth fronts, in particular, to the curved (200) crystalline planes in PE single crystals that have been both theoretically calculated [66,67] and experimentally observed [31,32]. In this case, a lattice strain in the {200} sectors was introduced into the HL theory, which was put into an independently justified surface free energy parameter. Molecularly 'serrated' (200) planes were also taken into account. Along the [110] direction, the crystal growth followed the standard HL theory for a smooth growth front [86,87].

Although regimes I and II of crystal growth in PE spherulites and axialites from the melt were experimentally observed in the mid 1970s, it took almost thirty years to quantitatively verify the existence of regime III growth in PE as shown in Fig. 4(a) and (b) [88]. Most of the experimental observations concerning polymer crystal growth rates can be explained by the HL theory. We will now summarize where the HL theory successfully describes the experimental observations of polymer crystal growth [89].

First, the HL theory was proposed to describe the isothermal crystal growth of a series of PE fractions in the melt at different T_cs. This theory was later utilized for many other semi-crystalline polymers to describe crystal growth

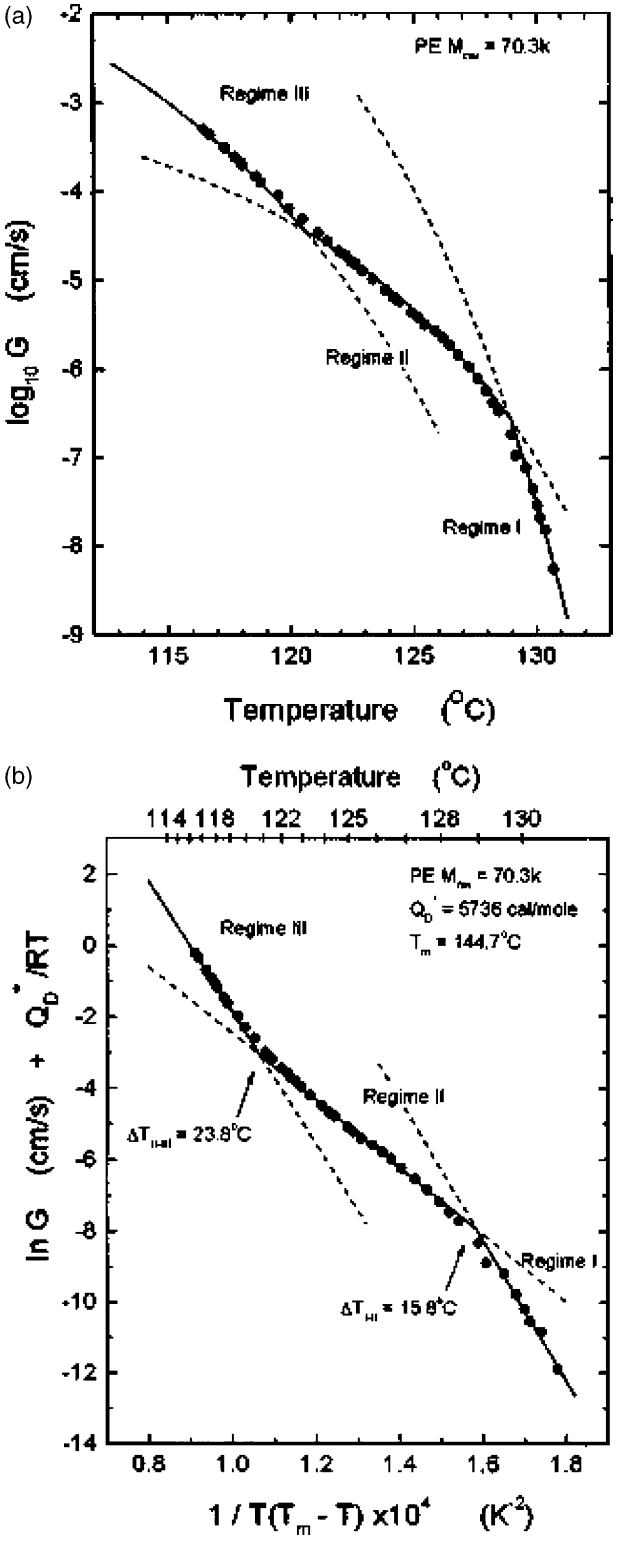

Fig. 4. Linear crystal growth rates of a PE fraction crystallized in the melt: (a) the experimentally measured growth rate data; and (b) three regimes after the experimental data were treated using the HL theory. Reprinted from [88] with permission.

behaviors as observed via PLM, AFM, and TEM, and to a lesser extent overall crystallization as measured by WAXD, dilatometry, and DSC experiments (this requires the athermal nucleation condition) [90–109]. As long as the spherulitic radial growth direction always follows a specific crystallographic plane normal and the growth is not affected by a local environment, the measured growth rates can be representative of lamellar single crystals along the specific growth direction. However, the ideal case would be to directly measure the growth rate of lamellar single crystals. This was achieved by either TEM, in situ AFM (for PE and st-PP) [31,32,42], or using a self-decoration method on single crystals [for poly(ethylene oxide) (PEO)] originally developed by Kovacs et al. [110–114], and later, applied by us [115].

Second, the lamellar thickness after crystallization is linearly proportional to $1/\Delta T$ for crystals grown in both the melt and solution [116]. The HL theory provided an analytical expression to illustrate this relationship. When the lamellar thickness is a constant, as in the case of growing extended chain crystals, the growth rate decreases linearly with respect to ΔT [117,118]. This was also analyzed by the HL theory [119].

Third, experimental observations reveal that in PE, along with many other semi-crystalline polymers, the crystal growth rates depend upon molecular weight (MW) [59,90, 94,120–128]. Therefore, using the HL theory to explain this MW dependence becomes critical. This was solved by introducing a MW dependent term into the pre-factor of the exponential equation of G in the HL theory [62,129].

Fourth, when a polymer sample having a broad MW distribution or a mixture with low and high MW fractions having identical chemical repeating units, molecular segregation of the low MW species takes place during crystallization [128,130,131]. The HL theory provided a qualitative explanation for this segregation phenomenon.

To summarize, the HL theory has been sufficiently fundamental in its assumptions to describe major crystallization phenomena for a wide range of semi-crystalline polymers. However, facing a variety of crystal growth behaviors and morphologies of these polymers reported, the HL theory has difficulties in providing explanations for several experimental observations. Some of 'overlooked' topics in this area were recently reviewed [132].

There are other proposed theories and approaches to describe polymer crystal growth. In order to explain molecular segregation in polymers with broad MW distributions, a molecular nucleation concept was proposed by Wunderlich [133]. A 2D nucleation process was suggested to describe molecular sliding diffusion along the *c*-axis in the PE hexagonal lattice at elevated pressures by Hikosaka [134,135]. An approach describing the rough surface growth of polymer crystals was also proposed by Sadler which parallels the growth mechanism of continuous crystallization of small molecules [136–142]. Although this approach initially ignored the chain connectivity in its simulations, an entropy barrier in polymer crystal growth was introduced, and the concept of a 'poisoning' mechanism was suggested based on the experimental observations of crystallizing *n*-alkanes [82]. For a critical description of polymer crystal growth, an excellent and extensive review was published by Armitstead and Goldbeck-Wood in 1992, and this remains one of the most thorough and important documents in this area [143].

3. What is the nucleation barrier in polymer crystal growth?

In the HL theory, the nucleation barrier concept is essential to understanding the mechanisms dominating polymer crystallization. It was originally solely of enthalpic origin, based on the competition between the bulk free energy and surface free energies when the initial crystal nucleus size is small. In the past twenty years, an entropic contribution to the nucleation barrier has been proposed and experimentally recognized in addition to the enthalpic contributions to the nucleation barrier. There are two major experimental approaches that can be used to understand the polymer crystallization. The first approach is from structural and morphological analysis. Although we cannot monitor every molecular trajectory to 'see' its dynamic pathway during crystal growth, it is though that the resulting polymer crystal structure and morphology have embedded pieces of this information and thus, provides insight about what happened during the nucleation and crystal growth processes. This approach uses structure and morphology as probes to logically deduce explanations concerning crystal growth on the sub-nanometer to nanometer scale, yet relies on the assumption that the final observed structure and morphology are true representations of the detailed consequences of the crystal growth process. The other approach is based on the results observed via scattering experiments. Since the scattering results represent an overall average of some types of density fluctuations in a system and they can be conducted as in situ measurements, the scattering results should represent what is happening during crystal growth. This viewpoint requires detailed microscopic models assisted by theoretical descriptions to explain the scattering experimental data. We have been working with ordered polymeric structures and morphologies for many years, and hence we utilize the structure and morphology point of view to analyze experimental observations on different length- and time-scales to elucidate the enthalpic and entropic origins of the nucleation barrier.

3.1. Chemical defect effect on nucleation barriers

It is the chemical and geometrical periodicities in crystals that provide the shortest length scale by which the nature of the nucleation barrier can be probed. Even in homo-polymers

with completely regular chemical structures where crystallization can take place, their crystallinity does not reach 100% (see previous sections for the discussion). When a polymer contains chemical defects, these defects must be rejected from the crystals as long as they are sizable and cannot be accommodated by the crystal lattice. Only small sized defects may be included in the crystals. Thermodynamic descriptions of defect exclusion [144] and inclusion [145] in the crystal were proposed (see also Ref. [146]). A known example is linear PE containing short-chain branching. When the short-chain branches are methyl groups, this defect may still be included in the PE orthorhombic crystal lattice. With increasing methyl group content, polymers gradually loose their ability to crystallize as the methyl content reaches ~20%. If short-chain branches on the comonomers increase in size to 1-butane, 1-hexyane, 1-octane, the crystallization is even more severely hampered and the polymer will remain as the corresponding amorphous elastomer at a lower level of short-chain branch content [147].

It has been illuminating to investigate the crystallization behavior of the systems containing certain degrees of chemical defects, yet can still crystallize [108,148–150]. As an example, Fig. 5(a) shows the linear crystal growth rates for a series of PE containing varying 1-octane comonomer content which is excluded from the PE crystal lattice [108]. As this content is increased, the growth rates substantially decrease. The exclusion of the short-chain branches formed by the comonomers of 1-butane, 1-hexyane, or 1-octane in it-PP copolymers has been extensively reported [151–154]. Case examples can also be found for the inclusion process. Crystal growth rate changes have been found in a series of it-PP with different isotacticities (so-called 'stereo-copolymers') [155–157] and it-PP copolymerized with ethylene units which are smaller than the propylene unit [151–154]. Fig. 5(b) shows growth rate data for a series of it-PP with different isotacticities. With decreasing isotacticity, the growth rates are significantly reduced, while the structural analysis indicated that the stereo-defects of it-PP are included in the crystals [156]. Although some of these samples may contain non-random distributions of the defects within the chains and between chains which affect the crystal growth rates, the predominant decreases of the growth rates with increasing defect content in the former case is the exclusion of defects from the crystal lattice, while in the later case is inclusion of the defects in the crystal lattice. Both observations indicate that any defect units in the chain molecules that deposit onto the crystal growth front hamper the crystal growth rates. This is because crystal growth requires that the defect be removed from the crystal front (exclusion), or form a non-crystalline spot on the growth surface as a point defect (inclusion). Both of these mechanisms slow down the growth rates and contribute to the nucleation barrier. This happens on the length scale of a fraction of a nanometer.

3.2. Stem conformational effect on nucleation barriers

The next length scale important to polymer crystallization is that of the stem conformation which is on the length scale of a few nanometers. For example, crystalline vinyl polymers exhibit helical stem conformations in crystals. In these polymers, the helical conformation of the stems, which are chiral but racemic, can possess either right or left-handedness. In addition, the substituent groups in vinyl polymers are usually tilted to the main chain axis rather than normal to it, which defines 'up' and 'down' orientations of the helices. As a result, a semi-crystalline vinyl polymer, such as it-PP, has four 3_1 helical conformations with an identical rotational energy as calculated based on the rotational isomeric model of a single chain [158]. The question is: how do stems with two handednesses and 'up' and 'down' conformational senses pack into the crystal lattice during growth? Note that chain folding only alters the chain direction and therefore the 'up' and 'down' conformational sense, and does not change the helical handedness, if the chain keeps a uniform handedness.

When we examine the polymer crystal structures using ED and WAXD experiments, it is evident that the helical chain packing requires the precise arrangement of stems into either antichiral or isochiral packing schemes. If an antichiral packing is necessary, a right-handed helical stem alternates with left-handed helical stems. On the other hand, isochiral packing requires that all the stems possess identical handedness in a crystal structure. Therefore during the crystal growth of a semi-crystalline vinyl polymer, the deposition of an initial part of the stem with the wrong helical handedness onto the growth front has to be rejected by the crystal lattice. The chain packing model of the it-PP α-form with its monoclinic lattice is shown in Fig. 6(a). Note that the stem handedness is alternating along the *b*-axis of the unit cell, which is a specific case in crystal packing with a coordination number of five. The arrangement of the 'up' and 'down' orientation of the methyl groups leads to two variants of the α-form, the α_1- and α_2-forms (Fig. 6(b) and (c)). Although the handedness packing in these two sub-forms is identical, the difference is that in the α_1-form, the 'up' and 'down' arrangement is random, while in the α_2-form, it is strictly alternating. This leads to two different space groups, $C2/c$ and $P2_1/c$, for these two sub-forms [159–165]. When an initial part of the helical stem with the wrong handedness gets deposited, one of two things could occur; it could undergo a conformation transition to correct its handedness, or be rejected back into the melt (or solution) [166–168]. For the specific case of it-PP, a third possibility exists, but only on the lateral ac growth front. It could rotate 100° (or 80°) to initiate a so-called 'lamellar branching' of the α phase or initiate the γ phase. Stems with the wrong 'up' or 'down' arrangement cannot be corrected in the solid state. Since the choice of the 'up' or 'down' arrangement requires time, the

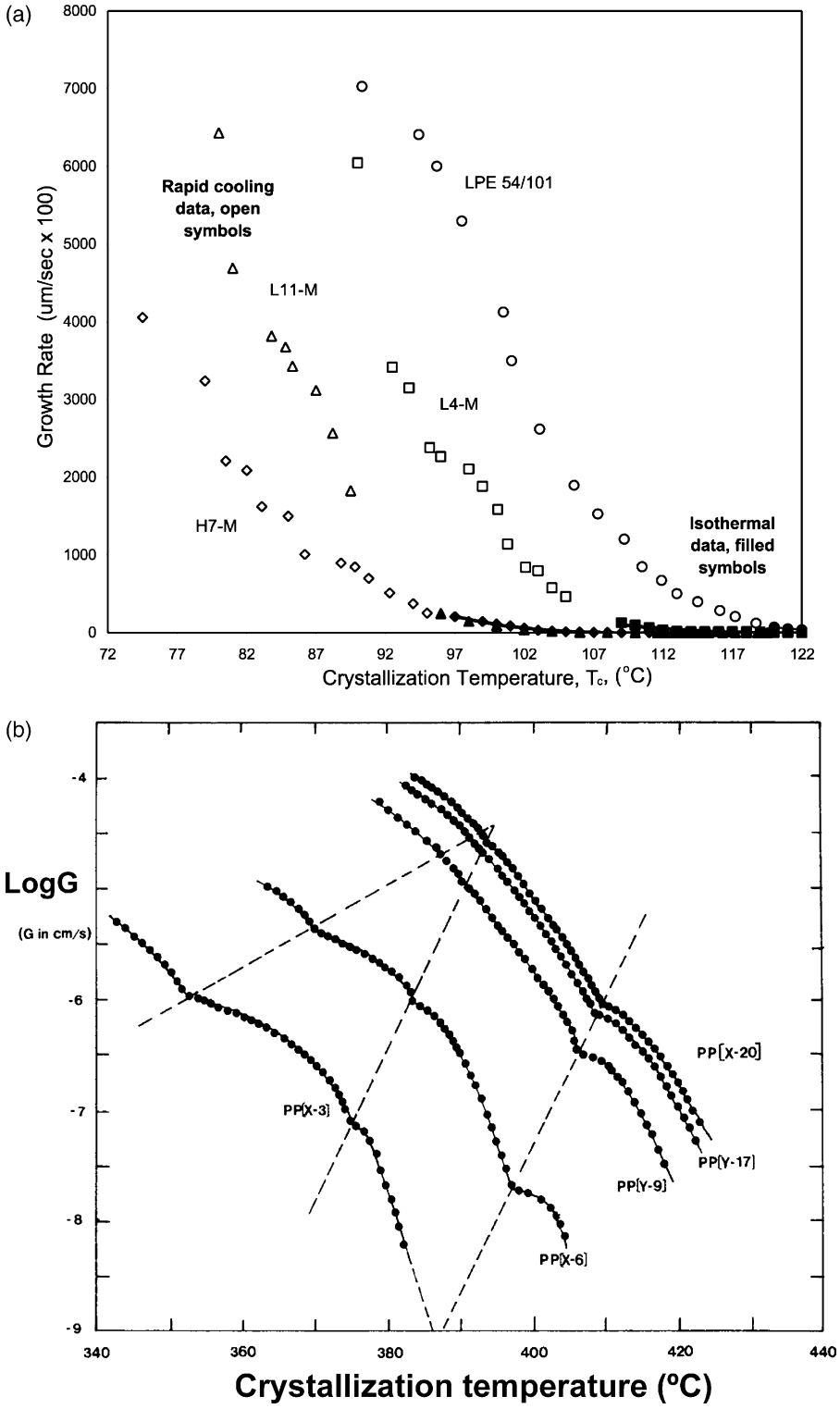

Fig. 5. A set of linear crystal growth rates of PE having different compositions of 1-octene as comonomer (a) from right to left, the crystal growth rate curves represent the data obtained from the samples of LPE-54/101 (linear), L4-M (3.98 per 1000 carbons), H7-M (6.84 per 1000 carbons), and L11-M (10.86 per 1000 carbons), while L and H refer to low and high MW, respectively. Note that the crystal growth rates not only depend on the comonomer content but also the MW. Reprinted from [108] with permission. A set of linear growth rates of it-PP with five different isotacticities in a wide T_c range (b) from the top to bottom, the growth rate curves represent the isotacticities of 98.8% PP(X-20), 97.8% PP(Y-17), 95.3% PP(Y-9), 88.2% PP(X-6) and 78.7% PP(X-3), respectively. Reprinted from [156] with permission.

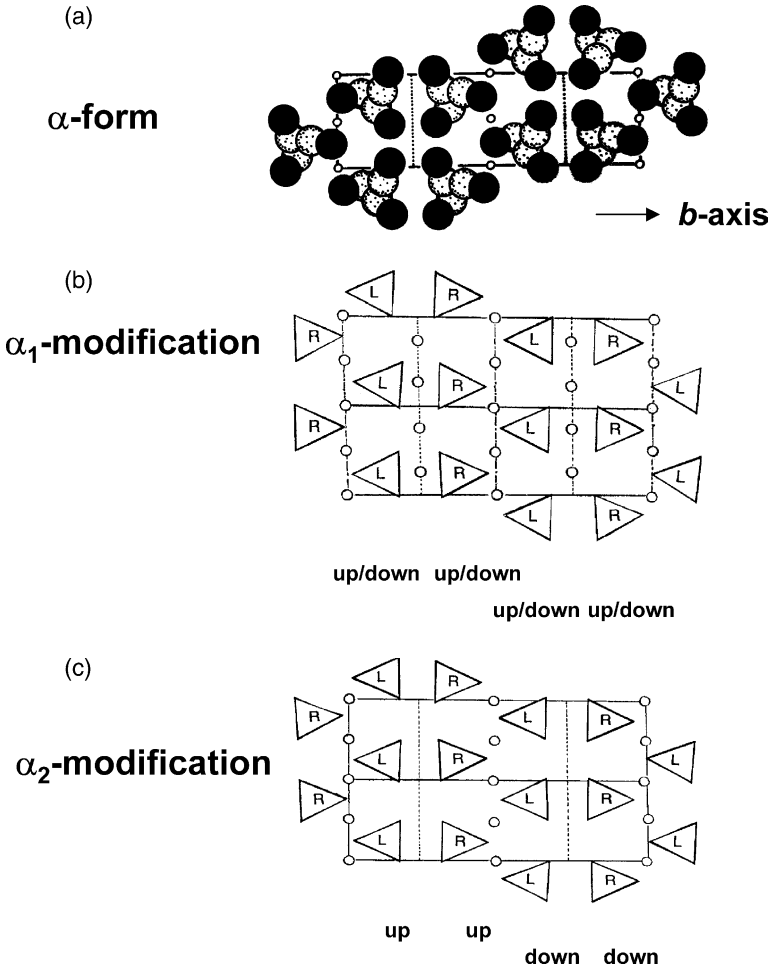

Fig. 6. A molecular packing model of it-PP α-form (monoclinic structure) with the unit cell dimensions of $a=0.666$ nm, $b=2.078$ nm, $c=0.646$ nm and $\beta=99.62°$. In this drawing, only the 'up' methyl groups are shown for simplification. Reprinted from [21] with permission (a); the α_1-form with random arrangement of 'up' and 'down' conformations (b); the α_2-form with an alternating arrangement of 'up' and 'down' conformations (c). Note their different space groups in the α_1- and α_2-forms.

α_2-modificaion can only grow at low ΔTs with slow growth rates. Another example is the crystal growth in it-PS, which possesses a 3_1 helical conformation and packs into a trigonal lattice with the $R\bar{3}c$ space group [169]. This symmetry operation contains both glide planes and centers of symmetry. Like many other 3_1 helical stems in the trigonal lattice, alternating handedness of the layers along the a-axis indicates clearly that during the crystal growth, handedness is one of the most important crystallographic requirements to fulfill. This serves as a general crystal packing scheme for all the semi-crystalline vinyl polymers.

When crystal growth takes place at high ΔTs, where the ΔG_η is still not a dominant factor, polymer crystal growth rates are generally fast. As a result, initial parts of the stems with the wrong conformation deposited onto the growth front may not have enough time to be corrected or rejected. This causes those inevitable 'mistakes' to be included into the crystal as long as the lattice can still accommodate them. Note that a single C–C conformational transformation takes place on the order of pico-seconds. A series of sequential transformations in the solid state to correct the handedness may require longer times. When these sequential transformations cannot keep up with the crystal growth rate, in the case of it-PP, a so-called 'smectic' phase forms from the melt [170]. In order to correct these conformational handedness defects, this 'smectic' phase needs more than 18 months at room temperature to carry out these corrective conformational transformations [171]. In the case of it-PS, it crystallizes into small ordered clusters of gels when it crystallizes in solution [172,173]. Computer simulations indicate that correction of handedness may be possible in it-PP crystals, but not in it-PS crystals since the substituent group is too big [174]. This inability to carry out conformational transitions in it-PS crystals was considered to be in part responsible for its very slow crystal growth rates [174]. Although a number of reports have appeared to describe the correction processes of stem conformations via thermal processes, such as metastable crystal annealing, pre-melting, and/or re-crystallization in semi-crystalline polymers, quantitative studies have yet to be awaited due to

the lack of a probe to directly detect the stem conformation and the difficulty of monitoring the correction processes.

One of the most convincing evidences for the selection process of stem conformation during the crystal growth is bio-degradable poly(L-lactide) (PLLA) and poly(D-lactide) (PDLA), which are chiral but non-racemic polymers, since the handedness of their helical conformations is fixed. When PLLA or PDLA crystallizes, both of them form the identical orthorhombic lattice with a P_{212121} space group [175,176]. The crystals of PLLA or PDLA contain only left- or right-handed helical stem conformation in strictly isochiral packing within a lozenge single crystal habit. However, stereo-complexes can also be formed using a PLLA/PDLA mixture with a composition ratio of 0.5:0.5. The resulting anti-chiral crystal lattice is trigonal with a space group of either $R3c$ for isocline helices or $R\bar{3}c$ for statistical 'up' or 'down' orientation of the helices [177]. The single crystal morphology is in a hexagonal shape.

Overall, these examples clearly illustrate that the single crystal habit does embed the handedness information of the stems during the crystal growth. The selection process of the helical handedness to create the lattice packing scheme is absolutely precise. Any mistakes made during the deposition process need to be corrected, and this correction process has to be a part of the nucleation barrier in crystal growth.

3.3. Lamellar thickness and global conformation effects on the nucleation barrier

On the order of tens of nanometers, lamellar single crystals are the building blocks of further crystal aggregates, and lamellar thickness is a specific characteristic that represents crystal stability and helps test theories. For all semi-crystalline polymers, lamellar thickness has been quantitatively understood to be proportional to $1/\Delta T$. However, the question still remains: why is lamellar thickness ΔT-specific? Here, we follow the explanation proposed by Armistead and Goldbeck-Wood [143]. Kinetic theories presume that the growth front would have a range of possible lamellar thicknesses, each of which possesses a corresponding growth rate. The observed thickness for the crystal is that which allows the crystal to grow the fastest and thus, is kinetically preferred (the fundamentally kinetic origin of the model). Including the HL theory, all the kinetic theories must possess two balanced factors, the 'driving force' for polymer crystal growth and the 'barrier'. The 'driving force' is determined by the penetration depth (ΔT) of the metastable liquid. At a given ΔT, this 'driving force' also depends on the lamellar thickness, l, which determines the stability of the crystal. When $l < l_{min}$, no crystal growth will take place because the crystallization inhibiting surface free energies overwhelm the crystallization promoting bulk free energy. When $l > l_{min}$, the bulk free energy starts to dominate causing the lamellae to grow thicker, since the γ_e is always larger than the γ in polymer crystals. The process accelerates as the thicker lamellae provide a stronger 'driving force', based on thermodynamics, until the 'driving force' approaches a constant as the effect of surface free energy becomes increasingly smaller. Therefore, if we only had the 'driving force' to determine the crystal growth, the fastest crystal growth rate would correspond to crystals with infinite thickness. However, there is another factor that needs to be taken into account. The 'barrier' must be overcome by means of a random fluctuation as a molecule deposits onto the crystal growth front. This barrier increases with lamellar thickness and thus, inhibits the formation of thicker crystals. The origin of this 'barrier' is thus the starting point for various kinetic theories [143].

Both the 'driving force' and 'barrier' together determine the growth rates which result from a compromise between the two factors as shown in Fig. 7 [143]. The thickness that corresponds to the maximum growth rate is slightly above l_{min} and thus, it is the underlying dependence of $l_{min} \propto 1/\Delta T$ as experimentally observed. The lamellar thickness is usually detected by small angle X-ray scattering (SAXS), TEM, AFM and in some cases such as in PE, it can be deduced using infrared and longitudinal acoustic mode Raman spectroscopy [178].

On the other hand, in the cases of *n*-alkanes and oligomers, so-called integral chain folding (IF) lamellar crystals grow, which exhibit a quantized increase of lamellar thickness with decreasing ΔT [110–114,179–182]. We now know that this is the result of annealing the non-integral chain folded (NIF) crystals [82,183–191]. The thickness of these NIF crystals also follows the linear relationship to $1/\Delta T$ [188]. Since the thermodynamic driving force to anneal NIF crystals into IF crystals in the solid diminishes and the activation barrier for cooperative

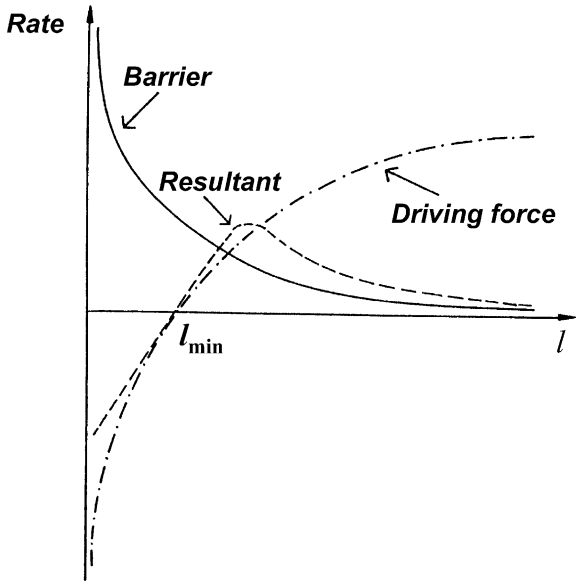

Fig. 7. The resultant growth rate which is determined by a compromise between the 'driving force' and nucleation barrier terms at a constant ΔT. Reprinted from [143] with permission.

molecular motion along the *c*-axis increases with increasing MW, increasing the MW of these oligomers and *n*-alkanes forces the NIF crystals to be permanently metastable [188]. Therefore, the thickness of high MW polymers shows a continuously linear relationship with $1/\Delta T$. This view certainly unifies the understanding of the crystallization in short and long chain molecules.

In addition to the enthalpic origin of the nucleation barrier, the crystal growth kinetics and morphological changes of the *n*-alkanes and other oligomers also provide important experimental evidence for the entropic origin of the nucleation barrier. When the *n*-alkanes crystallize into IF crystals at low ΔTs in the vicinity of the transition between the growth of the IF(n) (in most cases, $n=1$) and IF($n-1$) (extended) crystals, both crystal nucleation and growth rates exhibit a minimum for *n*-alkanes between $C_{162}H_{326}$ and $C_{294}H_{590}$ in the melt and solution crystallization [82,183,192–201]. A weak minimum in the single crystal growth rates of low MW PEO having methoxy end groups in the melt was also reported in the vicinity of the ΔTs where the growth changes from the IF($n=1$)→IF ($n=0$) crystals [115]. The explanation of the 'rate minimum' observations is that when a chain molecule with a folded IF(n) conformation deposits onto a crystal growth surface that prefers to grow the IF($n-1$) crystal, this location becomes 'poisoned' to hamper the IF($n-1$) crystal growth. Further crystal growth requires the correction of this 'mistake' by either extending the folded conformation or removing this chain to release this 'poisoned' spot. Therefore, both the nucleation and growth rates decrease. This is called 'self-poisoning' because the mistake was made by the chain molecule itself [82,183,192].

In order to elaborate on this concept, blends of two *n*-alkanes having different MWs showed that the growth of longer *n*-alkanes was 'poisoned' by depositions of the shorter molecules on the growth front, and this 'poisoning' also caused a 'rate minimum' to appear [200,201]. If we extend this concept to illustrate the crystallization behaviors of homo-polymers which consist of mixtures of two different MWs, as long as the MW of one component is low enough to be recognized by the crystal growth front, the deposition of this low MW polymer onto the growth front 'poisons' further growth and slows down the crystal nucleation and growth rates. This type of 'poisoning' may not generate an observable macroscopic 'rate minimum', yet the molecular selection in the growth process always exists. The molecular selection process has been observed in the binary mixtures of low MW PEO fractions with a high MW PEO fraction. The high MW PEO fraction crystallizes first but with much slower growth rates compared to the homo-PEO crystal growth rates at the same low ΔT values [130]. The low MW PEO fraction thus acts as a 'poisoning' agent and is rejected and segregated between lamellae (microscopic) and/or between spherulites (macroscopic) [131]. This molecular selection was also observed in the case of PE with a broad MW distribution in the melt and solution [202,203].

This type of 'poisoning' effect can also be observed in the stereo-complex of chiral PLLA and PDLA crystals as previously described. Extensive work has been conducted to evaluate the stem conformation selection process at this length scale [204,205]. When the MWs of the two polymers in the blend exceed about 4×10^4 g/mol, separate PLLA and PDLA crystals are grown. When the MWs of both PLLA and PDLA are lower than this value, they form stereo-complexes. Blending a high MW polymer with its low MW enantiomer also results in the formation of the stereo-complex. Diffusion processes to the growth front and the correct deposition of the helical conformations seem to play major roles in the molecular selection process associated with the crystallization of the stereo-complex.

One can find many experimental reports regarding this selection (or 'sorting out') process in the crystallization of miscible polymer blends with one crystallizable component [206–208]. When the crystalline component crystallizes, phase separation is induced. The probability of which component deposits onto the growth front depends on the local density of that component. The selection process takes place at the growth front, and only the crystallizable component can be used for crystallization. This significantly decreases the growth kinetics, and the non-crystallizable component is now 'poisoning' the crystal growth. Similar cases can also be found in the crystallization of crystalline-amorphous diblock copolymers in solution [209]. However, separation of enthalpic and entropic contributions is experimentally difficult.

3.4. Physical environment effect on polymer crystallization

During polymer crystallization, it was observed that enhanced growth rates can be achieved due to the re-entrant corners of twins [210,211], in particular, in both n-alkanes [212,213] and PE [214,215]. When PE single crystals grow in dilute solution, often twinning, such as a {110} twin, occurs. As shown in Fig. 8(a), the {110} twin constructs a 112.6° re-entrant corner, which enhances further PE crystal growth (note that during the growth the angle gradually increases due to the curvature of the {200} planes) [216]. This is due to the fact that the corner provides a less-than-180° growth front reducing the lateral surface free energy when the PE chain deposits at the corner, thus enhancing the growth rate. Based on calculations only taking the reduced lateral surface free energy into account, the growth rate at the corner should speed up by several orders of magnitude. However, experimental data showed that the enhancement is much less than that predicted by the theory [216]. The reduced enhancement may be due to the limited space in front of the corner in addition to other factors such as the lattice match at the corner. The geometric confinement thus plays a significant role in the crystal growth behavior.

When PE crystallizes in the melt at low ΔT_s, single

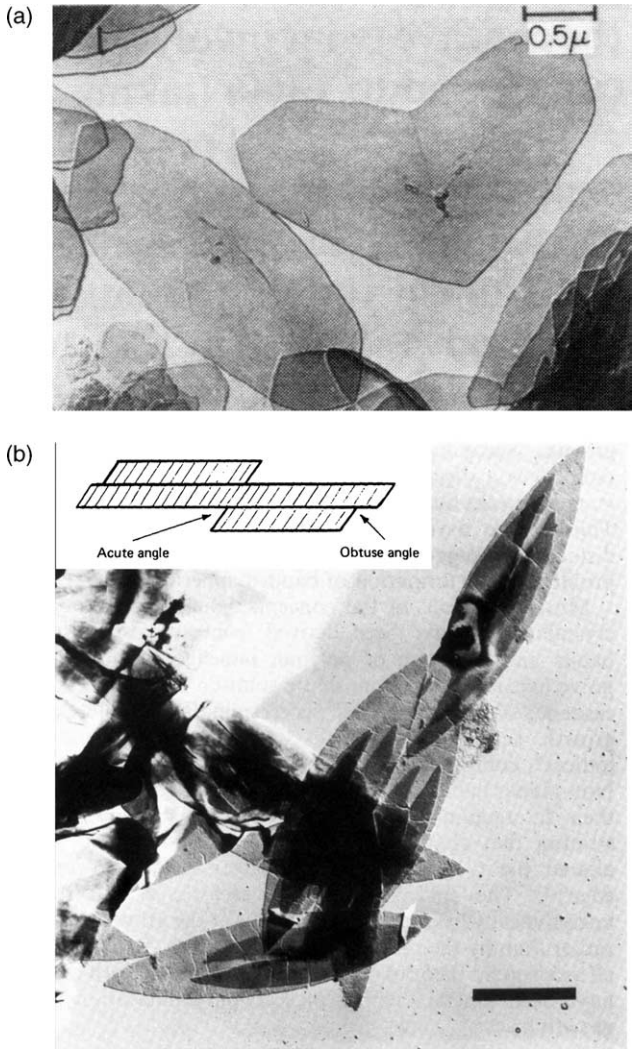

Fig. 8. Experimental observations of PE crystal growth at a reentry corner constructed by a (110) twin in solution. Reprint from [216] with permission (a); and an anisotropic crystal growth along the [200] direction of PE single crystals formed by screw dislocations on their mother PE single crystals in the melt. The insert illustrates the chain tilting effect on the crystal growth on both sides of the curved (200) planes (b). Reprint from [29] with permission.

crystals can grow as shown in Fig. 8(b) [29]. In this figure, the large mother single crystals that developed first possess a symmetrical lenticular-shape. Smaller daughter single crystals grown later due to screw dislocations possess a substrate on their bottom or top provided by the mother single crystal, and therefore, they have slower growth rates than their mother crystal due to confinement of the substrate. It is worth further noting that the shapes of these daughter crystals are asymmetric along the two opposite [200] directions, indicating that the growth rates along both the [200] directions are not equal. This inequality is due to the fact that the PE chains in the single crystals are tilted towards the [200] direction usually ranging between 20 and 35° with the highest tilting angle reported being 45°. This generates two growth fronts with one $<90°$ (acute) and another $>90°$ (obtuse) with respect to the substrate. Since the chains can more easily access the obtuse growth front, the growth rates along the [200] directions are thus affected by the difficulty of this deposition process [29].

Recently, active research has been conducted in the area of polymer crystallization in 1D, 2D and 3D nano-confined environments, which are created from templates of microphase separated crystalline–amorphous block copolymers [217–220]. The basic concept of this approach is to design block copolymers to control three transition processes: the order–disorder transition of the microphase morphology formation (T_{ODT}), the vitrification of the amorphous block (T_g), and the melting temperature of the crystalline block (T_m) [221]. Generally speaking, when the condition $T_{ODT} > T_g > T_m$ exists, a hard-confined environment in which crystallization can take place is created. If the condition $T_{ODT} > T_g \sim T_m$ exists, a soft-confined environment is formed [222]. But when the condition $T_{ODT} > T_m > T_g$ exists, the crystallization breaks the microphase morphology to achieve its own lamellar texture [223–225]. So far, all the studies show that the nano-confinement impedes overall crystallization rates coupled with the crystal orientation changes within the confined spaces. Furthermore, with increased dimensionality of confinement, the reduction of the crystallization rate becomes more severe. A very recent study showed that by releasing the 1D confinement in a precisely controlled way, the crystal orientation significantly changes [226]. These crystallization processes have been understood to be nucleation controlled even in the high ΔT region. Crystal lamellar thicknesses and melting of the diblock copolymers crystallized in the bulk and dilute solution have also been invested [227,228]. The results show that the crystalline lamellar thicknesses are determined by a balance of the entropic free energy near the lamellar surfaces created by the amorphous block repulsion and the crystal growth barrier of the crystalline blocks, as first theoretically proposed by DiMarzio et al. [229]. All the experimental observations indicate that the physical environments should also have an effect on the nucleation barrier.

3.5. Crystallization from the isotropic melt versus from a pre-ordered state

Most of investigations on polymer crystallization and growth are from the isotropic melt (or solution) in which the global chain conformations are random coils. The question is whether we can observe differences in the crystallization kinetics obtained from the melt and from a pre-ordered (*meso*-phase) state under a condition that the crystal structures after the crystallization from the isotropic melt and *meso*-phase are identical. Monotropic phase behavior in semi-crystalline polymers, where a metastable *meso*-phase exists, has provided a unique opportunity to study the differences in the overall crystallization and growth rates of

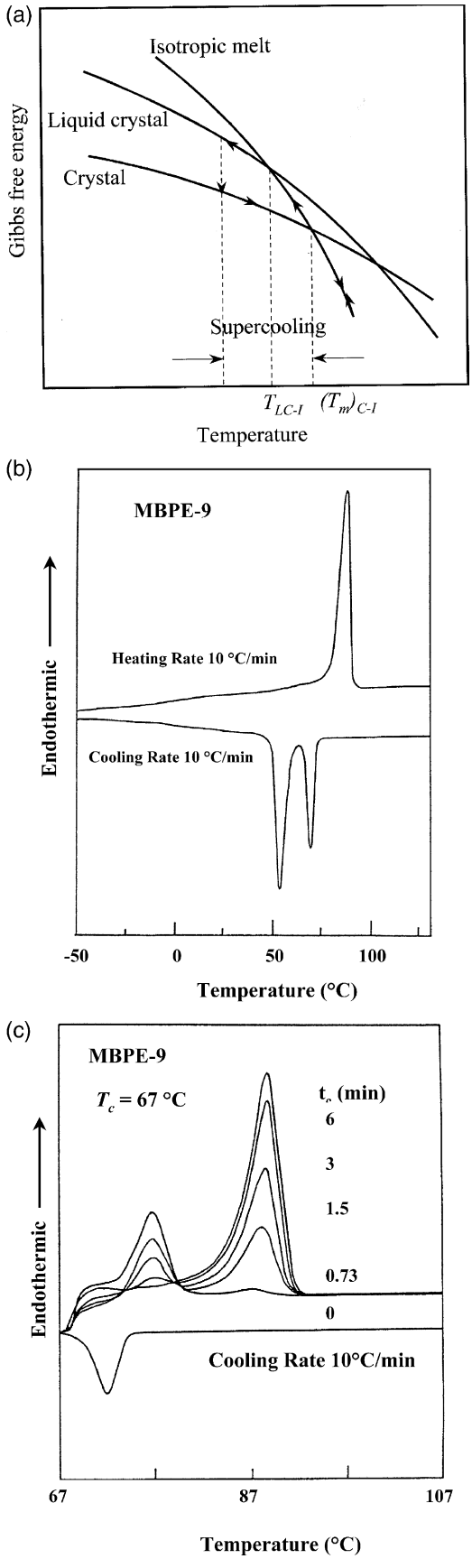

a polymer crystallizing from either the isotropic melt or the *meso*-phase.

Fig. 9(a) shows a phase behavior plot between the free energy and temperature at a constant pressure. In this figure, the *meso*-phase is metastable in the entire temperature region. This *meso*-phase can be accessed only under the condition that the stable crystal phase formation during cooling can be bypassed due to the need to overcome a nucleation barrier. If one cools the sample rapidly, the crystallization process is suppressed resulting in the formation of a *meso*-phase, since the metastable *meso*-phase transition is close to equilibrium with little ΔT, such as in the case of liquid crystalline (LC) phase formation. The crystallization then takes place from the *meso*-phase instead of the isotropic melt [230–238]. This type of monotropic LC behavior was first found in a series of polyethers made from a semiflexible mesogen, 1-(4-hydroxyphenyl)-2-(2-methyl-4-hydroxyphenyl)ethane (MBPE) [230–234]. Fig. 9(b) shows an example of this series of polyethers which exhibit a monotropic LC phase behavior in DSC cooling and subsequent heating experiments [233]. During cooling, an isotropic to LC phase transition at T_i (an isotropization temperature) can be observed before the polyether started crystallizing. The second exothermic process is the crystallization process. The subsequent heating shows that only one endothermic process can be found at a T_m higher than the T_i observed during cooling (Fig. 9(b)). If we cooled the sample to between these two exothermic peaks, annealed there for different times and then heated the sample to above its T_m without further cooling as shown in Fig. 9(c), the heating diagram without annealing recovers almost all of the enthalpic change of the LC phase at T_i during heating. After only 6 min annealing, the enthalpic change of the LC phase disappears, and the crystal melting dominates at T_m [233]. This indicates that very short annealing times could transform the LC phase to a crystal phase. The remaining LC phase, since polymers rarely reach 100% crystallinity, does not undergo isotropization in Fig. 9(b) due possibly to the confinement constructed by the newly formed crystals resulting in a superheated LC phase.

Let us now study the transition kinetics. In Fig. 10(a), overall crystallization rates of one of the monotropic

Fig. 9. A plot of Gibbs free energy with temperature at a constant pressure for a metastable state within the entire temperature region (a). Reprinted from [231] with permission. A set of DSC cooling and substantial heating diagrams at 10 °C/min for a polyether (MBPE) based on the semiflexible mesogen 1-(4-hydroxyphenyl)-2-(2-methyl-4-hydroxyphenyl)ethane. This series of MBPE polyethers possesses a monotropic LC phase. In this figure, the sample has nine methylene units in the backbones. During the cooling, the first exothermic peak is the formation of the metastable LC phase and the second exothermic peak is the crystallization. During heating, on the other hand, only the crystal melting can be observed by the single endothermic peak (b). A set of DSC heating diagrams after the MBPE polyether sample with nine methylene units cooling at 10 °C/min to slightly below the exothermal peak to form the mestastable LC phase and annealed at different times (c). Reprint from [230] with permission.

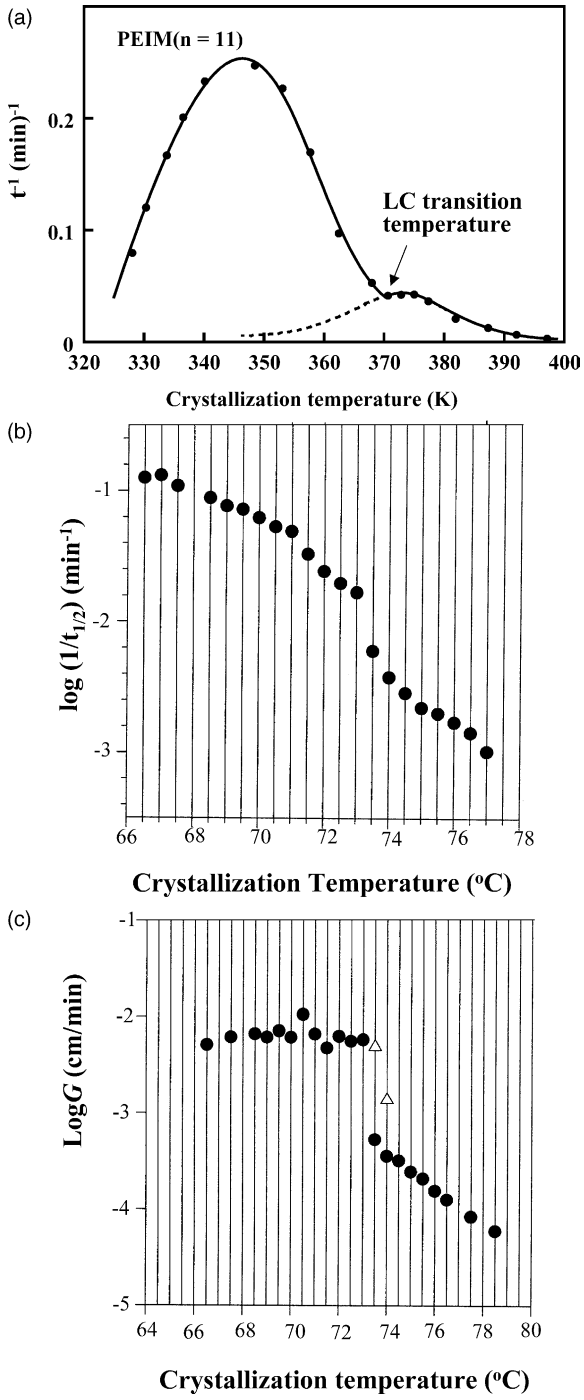

Fig. 10. Overall crystallization kinetics of a poly(ether imide) (PEIM) synthesized from *N*-[4-(chloroformyl)phenyl]-4-(chloroformyl)phthalimide and diols containing eleven methylene units is plotted with respect to isothermal temperature above and below the LC transition temperature at (a). Reprinted from [234] with permission. Crystal growth rates of a MBPE polyether above and below the LC transition temperature (b). Overall crystallization rates of a MBPE polyether above and below the LC transition temperature (c). Reprinted from [231] with permission.

poly(ester imide)s (PEIM) synthesized from *N*-[4-(chloroformyl)phenyl]-4-(chloroformyl)-phthalimide and diols containing 11 methylene units is plotted with respect to isothermal temperature [237]. The advantage of this example is that we can study the phase transition kinetics across the whole isothermal temperature region between T_g and T_m. In this figure, the existence of the LC phase, which has at least stem orientational order, substantially enhances the overall crystallization rates of the polymers compared with crystallization from the isotropic melt. Yet the crystal structures formed above and below the LC phase transition temperature are identical, as verified by WAXD experiments [237]. The question is whether this LC phase only speeds up the primary nucleation rate or also enhances the crystal growth rate. A recent study on a MBPE polyether with nine methylene units reported that both the overall crystallization (Fig. 10(b)) and crystal growth rates (Fig. 10(c)) were enhanced [234]. The enhancement of both the nucleation and growth rates in the pre-ordered state implies that both primary and surface nucleation barriers are reduced by introducing stem orientational order. This also indicates that the global chain conformations near and at the growth front during the crystal growth in the isotropic melt and the pre-ordered state are very different.

4. Issues remaining in polymer crystallization

As we have stated previously, the views described in this article are solely based on the structure and morphology observed experimentally with the assumption that the structure and morphology contains microscopic evidence of the nucleation and growth processes. Therefore, our microscopic analyses almost exclusively rely on solid state observations. We know much less about the structure of undercooled liquids during polymer crystallization. Polymer crystallization and melting are thermodynamic first-order transitions. In the description of a first-order transition between a gas and a liquid of a single component system in a pressure–volume phase diagram at different temperatures, two stability limits serve as boundaries. The first boundary is the binodal line which represents the phase stability limit, while the spinodal line is the phase metastability limit as shown in Fig. 11 [238]. Areas bounded between these two lines, the first-order transition takes place as a nucleation process, implying that we may have a superheated liquid or an undercooled gas phase within these pressure–volume areas. However, as soon as the spinodal line is reached, the metastable liquid or gas can no longer exist. Therefore, if we represent a first-order transition between liquid and gas phases by plotting free energy with respect to temperature at a constant pressure or with pressure at a constant temperature as shown in Fig. 12(a) and (b), the superheated liquid and undercooled gas or superexpanded liquid and supercompressed gas will reach the limit of metastability, and thus, possess two end points in these metastable states as shown in these two figures (filled circles in Fig. 12), which are defined by the spinodal line. For crystallization and melting which describe the solid and liquid transitions, the classical metastability limit presented in Fig. 12(a) and

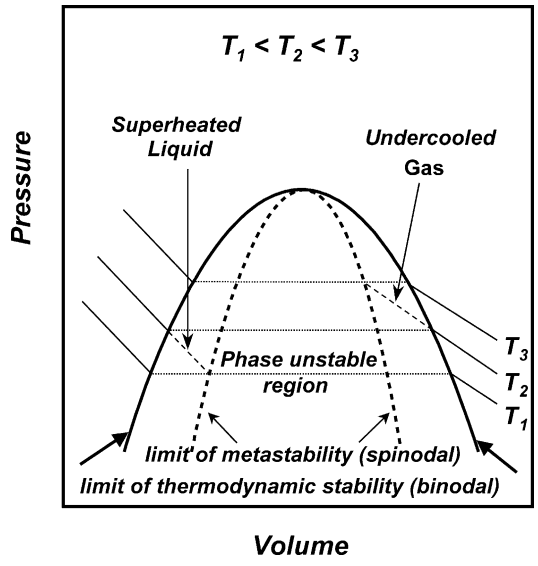

Fig. 11. A plot of the pressure and volume relationship at different temperatures for a liquid–gas system. Outside of the binodal line, a single phase is stable. Between the binodal and spinodal lines, the phase transition takes place in a metastable state. Within the spinodal line, the phase is unstable. Reprinted from [235] with permission.

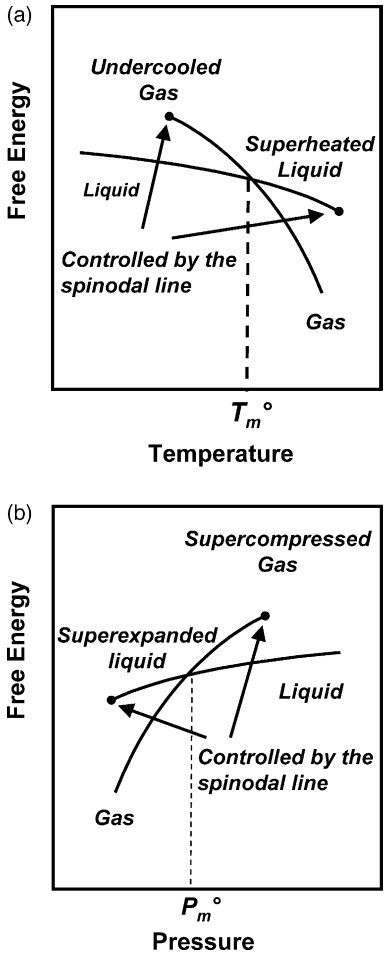

Fig. 12. Relationships between Gibbs free energy and temperature at a constant pressure (a), and Gibbs free energy and pressure at a constant temperature (b). For the liquid–gas transition, limits of metastabilities of liquid and gas can be defined by the spinodal line and therefore, the depths of the metastablities penetrating into both the gas and liquid phases are fixed (the filled circles in these figures). However, this is not the case for a liquid–solid transition (see text).

(b) does not exist, because neither the superheated crystal (or superexpanded crystal) nor the undercooled liquid (or supercompressed liquid) reaches the metastability limit of the spinodal line. The reason is that in the liquid–gas transition phase symmetries do not change, while in the crystal–liquid transition, phase symmetries drastically and suddenly change. Therefore, we describe the crystallization process as a relaxation of the metastable undercooled melt towards the equilibrium state by overcoming a free energy barrier. The height of this barrier depends on the depth of penetration into the metastable state (ΔT). In order to create a new phase in the metastable melt, interfaces must be introduced through the nucleation process. If the resulting nuclei are larger than a critical size, they will continuously grow towards a stable crystalline phase. According to the classical understanding of a single component system, the nucleation barrier of the melt-to-crystal transition never vanishes. As a result, no unstable liquid exists [238–242].

The remaining issues in polymer crystallization are associated with our understanding of the structure of metastable liquids and how the crystallization is initiated. These issues may critically rely on the experimental observations of scattering techniques. For semi-crystalline polymers, we have only limited structural understanding of their undercooled liquids with thermal fluctuation. When primary nuclei form in the metastable undercooled polymer liquids, how do the thermal fluctuations of the liquids trigger the primary nucleation as the initial stage of polymer crystallization? The recently proposed spinodal-assisted (primary) nucleation reflects the effort to understand this issue [243]. Different versions of this approach have also been reported [244,245]. A classical spinodal decomposition process describes how an unstable system relaxes by the spontaneous growth of long-wavelength fluctuations of small amplitude. This process does not require an energy barrier, and the density perturbations in single component systems and composition perturbations in mixtures are thought to be large in extent but small in intensity. For polymer crystallization with an identical chemical repeating unit and nearly equal chain length like a single component system, can the spinodal-assisted nucleation process exist in an undecooled liquid? Recent computer simulation results do not support this mechanism [246,247].

The primary nucleation process in polymer crystallization is understood much less than the crystal growth process, although investigations were started with the help of droplet experiments in the late 1940s [248]. In general, the density of homogeneous nucleation increases with increasing ΔT. Recent reports on primary nucleation in PEO droplets generated by de-wetting PEO films on a PS

substrate provided a new methodology to investigate the homogeneous nucleation in semi-crystalline polymers and yielded some interesting results [249,250]. An important experimental observation was made for slow crystallizing polymers such as it-PS, which can rapidly be quenched to below its T_g without crystallization. This quenching process freezes the thermal fluctuations in the polymer melt. Thermal aging below T_g affects the subsequent overall crystallization process when the samples were brought back to a temperature between T_g and T_m. Fig. 13 shows that the growth rate is barely, or not affected at all in the it-PS samples regardless of their thermal histories (directly quenched from the melt or after thermal aging below the T_g). On the other hand, the crystallization half-time is reduced by one decade of time after the samples were thermally aged compared with the sample directly quenched from the melt. This increase in overall crystallization rate results mainly from an increase in primary nucleation density by nearly three orders of magnitude (but part of it may be due to 'homogeneous' nucleation taking place slightly above T_g, during the cooling process). Furthermore, expanding the aging time below T_g results in a 10 fold increase in the nucleation density between 6 and 15 min [251]. The latter observation indicates that although the large-scale thermal fluctuations had been frozen below T_g, the local densifications contribute to the formation of primary nucleation. The questions which remain are how does the local densification develop during aging within the frozen large-scale thermal fluctuation in an undercooled liquid below T_g? and What role does denser packing in the amorphous phase play in enhancing the primary nucleation?

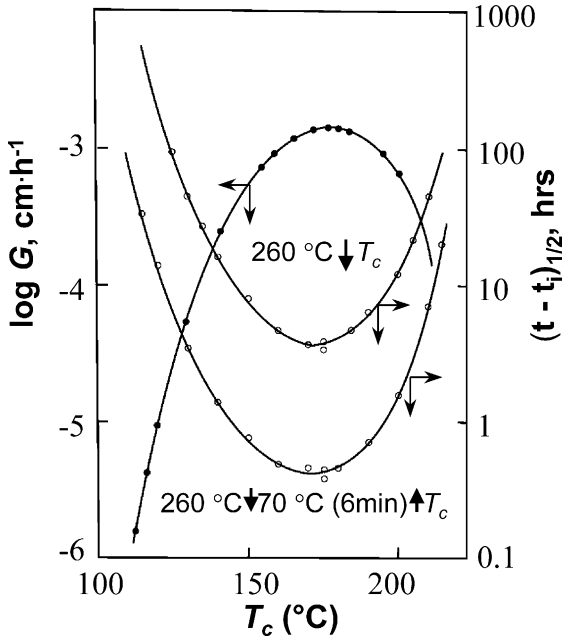

Fig. 13. Relationships between the linear crystal growth rates (observed using PLM) and the overall crystallization half-time to reach full crystallinity (observed in DSC) of it-PS samples with T_c with two different thermal histories: one is the it-PS samples were directly quenched from the isotropic melt at 260 °C to different T_c; and another is that the samples were first quenched to a 70 °C (which is 30 °C below the T_g of it-PS), and then annealed there for 6 min. The samples with both thermal histories were then used to measure their crystal growth rates and overall crystallization rates.

For polymer crystal growth, the structure of the interfacial liquid near the growth front is also not clearly understood. Recent efforts on this issue suggest that the liquid phase near the crystal growth front is in a mesomorphic phase, and that polymer lamellar crystals form via a pathway in which granular crystals form first, and then these granular crystals connect with each other to construct a lamellar crystal [252]. Some AFM micrographs were shown to support this view. This issue reflects the difference in attempting to understand polymer crystal growth from the structural and the scattering points of view [167,252–254]. In addition to the observations we have discussed in Section 3.5, recent experimental results in very fast DSC experiments with cooling and heating rates exceeding several thousand degrees per second showed that the recrystallization process during heating after melting is substantially faster than the crystal growth from the original isotropic melt [255]. Does this indicate that even shortly after crystal melting, the global chain conformations are still far from a completely random coil and thus, recrystallization becomes a process of crystallization from a phase which retains some degree of stem orientational order? It would be very interesting if this study can be extended to semi-crystalline polymers with racemic helical chain conformations in their crystals.

5. Conclusion

It was the aim of this article to briefly review the HL theory of PE crystal growth and its application to other polymers. The HL theory has so far remained the major analytical 'mean-field' approach and has had a profound influence in the area of polymer crystallization. We have summarized the major experimental observations concerning crystal growth kinetics and their relationships with crystal morphology to show that the HL theory is flexible enough to accommodate some of these experimental observations. The HL theory and experiments presently available provide the basis for looking ahead and trying to find pathways to gain further insight into the polymer crystal growth process. From a broader perspective, we have introduced a new look at the nucleation barrier. The multiple selection processes on different length- and time-scales that take place during crystallization give rise to experimental probes that can be used to monitor their effects on the nucleation barrier. The selection rules depend on the similarity of each structural, molecular, or morphological unit that was probed in different length scales. The less similarity in the structural, molecular, or morphological unit results in a stronger 'sorting out' process. The combination

of these processes creates a nucleation barrier that includes both enthalpic and entropic contributions. Statistical mechanics is necessary to connect these microscopic contributions to the nucleation barrier which is commonly described by classical thermodynamics. Although our understanding of solid state structures has progressed significantly, the issues remaining concern the structure and dynamics of the undercooled melt along with the structure and dynamics of the liquid near the interface, and their association with nucleation and growth processes.

Acknowledgements

Both of the authors are indebted to many coworkers and colleagues, too numerous to be cited, for valuable input into the development of the ideas expressed in this contribution. The authors would like to dedicate this article to the late Professor John D. Hoffman, who played the major role in different periods of the authors professional careers. The authors would like to sincerely thank Dr Freddy Khoury, Prof Phil H. Geil and Prof Buckley Crist for their thoughtful and helpful comments. SZDC acknowledges the support of NSF (DMR-0203994 and 0516602).

References

[1] See, for example, Volmer M. Kinetik der Phasenbildung. Dresden: Steinkopff; 1939 and the references cited.
[2] Turnbull D, Fisher JC. J Chem Phys 1949;17:71.
[3] Rosenberger F. Crystal growth kinetics. In: Mutaftschiev B, editor. Interfacial aspects of phase transformations. Proceedings of the NATO advanced study institute. Dordrecht: Reidel Publishing Company; 1982. p. 315–63.
[4] Hermann K, Gerngross O, Abitz W. Z Phys Chem 1930;B10:371.
[5] Jaccodine R. Nature 1955;176:305–6.
[6] Keller A. Philos Mag 1957;2:1171.
[7] Till Jr PH. J Polym Sci 1957;24:301–6.
[8] Fischer EW. Z Naturforsch 1957;12a:753.
[9] Kobayashi K. Kobunshi no Bussei (properties of polymers). In: Nakajima A, Tadokoro H, Tsuruta T, Yuki H, Ohtsu T, editors. Kyoto: Kagakudojin; 1962. p. 203–20, chapter 11.
[10] Storks KH. J Am Chem Soc 1938;60:1753.
[11] Point JJ. Bull Acad R Bel 1953;41:982.
[12] Keith HD, Padden Jr FJ. J Polym Sci 1959;39:123.
[13] Keller A. J Polym Sci 1959;39:151.
[14] Price FP. J Polym Sci 1959;39:139.
[15] Wunderlich B, Sullivan P. J Polym Sci 1962;61:51.
[16] Fischer EW, Lorenz R. Kolloid Z Z Polym 1963;189:97.
[17] Wunderlich B, James EA, Shu SW. J Polym Sci 1964;2:2759.
[18] Khoury F. J Res Natl Bur Stand 1966;70(A):29.
[19] Geil PH. Polymer single crystals. New York: Wiley-Interscience; 1963.
[20] Keller A. Rep Prog Phys 1968;31:623.
[21] Wunderlich B. Macromolecular physics. Crystal structure, morphology, defect, vol. 1. New York: Academic Press; 1973 [chapter 2].
[22] Khoury F, Passaglia E. The morphology of crystalline synthetic polymers. In: Hannay NB, editor. Treatise on solid state chemistry, vol. 3. New York: Plenum; 1976. p. 335–496 [chapter 6].
[23] Bassett DC. Principles of polymer morphology. Cambridge: Cambridge University Press; 1980.
[24] Cheng SZD, Li CY. Mater Sci Forum 2002;408:25.
[25] The pioneering work on elongated PE single crystals grown in poor solvents is due to Khoury F. Faraday Disc Chem Soc 1979;68:404. Khoury F. Scanning transmission electron microscopy of polyethylene crystals. 38th annual proceedings, Electron Microscopy Society America, 1980. p. 242–5. Khoury F, Bolz L. Bull Am Phys Soc 1985;30:493. Subsequent work by Prof A. Keller, inspired in part by these early results, led to the publications cited as Refs. [26–28].
[26] Organ SJ, Keller A. J Mater Sci 1985;20:1571.
[27] Organ SJ, Keller A. J Mater Sci 1985;20:1586.
[28] Organ SJ, Keller A. J Mater Sci 1985;20:1602.
[29] Bassett DC, Olley RH, Al Raheil AM. Polymer 1988;29:1539.
[30] Keith HD, Padden Jr FJ, Lotz B, Wittmann JC. Macromolecules 1989;22:2230.
[31] Toda A. Colloid Polym Sci 1992;270:667.
[32] Toda A, Keller A. Colloid Polym Sci 1993;271:328.
[33] Toda A. Disc Faraday Soc 1993;95:129.
[34] Sauer JA, Morrow DR, Richardson GC. J Appl Phys 1965;36:3017.
[35] Wittmann JC, Lotz B. J Polym Sci, Polym Phys Ed 1985;23:205.
[36] Lotz B, Graff S, Straupe C, Wittmann JC. Polymer 1991;32:2902.
[37] Lotz B, Lovinger AJ, Cais RE. Macromolecules 1988;21:2375.
[38] Lovinger AJ, Davis DD, Lotz B. Macromolecules 1991;24:552.
[39] Lovinger AJ, Lotz B, Davis DD. Polymer 1990;31:2253.
[40] Lovinger AJ, Lotz B, Davis DD, Padden Jr FJ. Macromolecules 1993;26:3494.
[41] Bu Z, Yoon Y, Ho RM, Zhou W, Jangchud I, Eby RK, et al. Macromolecules 1996;29:6575.
[42] Zhou WW, Cheng SZD, Putthanarat S, Eby RK, Reneker DH, Lotz B, et al. Macromolecules 2000;33:6861.
[43] Zhou WW, Weng X, Jin S, Rastogi S, Lovinger AJ, Lotz B, et al. Macromolecules 2003;369485.
[44] Briber RM, Khoury FA. J Polym Sci, Polym Phys Ed 1993;31:1253.
[45] Toda A, Arita T, Hikosaka M. Polymer 2001;42:2223.
[46] Bassett DC, Turner B. Nature 1972;240:146.
[47] Di Corleto JA, Bassett DC. Polymer 1990;31:1971.
[48] Geil PH, Symons NKJ, Scott RG. J Appl Phys 1959;30:1516.
[49] Khoury F, Barnes JD. J Res Natl Bur Stand 1974;78A:95.
[50] Keith HD. J Polym Sci Part A 1964;2:4339.
[51] Keith HD, Padden Jr FJ. J Polym Sci, Polym Phys Ed 1987;25:2371.
[52] Frank FC, Keller A, O'Connor A. Philos Mag 1959;4:200.
[53] Bassett DC. Philos Mag Ser VIII 1964;10:595.
[54] Bassett DC, Dammont FR, Salovey R. Polymer 1964;5:579.
[55] Khoury F, Barnes JD. J Res Natl Bur Stand 1972;76A:225.
[56] Patel D, Bassett DC. Proc R Soc London A 1994;445:577.
[57] Ho RM, Lin CP, Hseih PY, Chung TM, Tsai HY. Macromolecules 2001;34:6727.
[58] Hoffman JD, Lauritzen Jr JI. J Res Natl Bur Stand 1961;65A:297.
[59] Lauritzen Jr JI, Hoffman JD. J Appl Phys 1973;44:4340.
[60] Hoffman JD, Frolen LJ, Gaylon SR, Laurizen Jr JI. J Res Natl Bur Stand 1975;79A:671.
[61] Hoffman JD, Davis GT, Lauritzen Jr JI. The rate of crystallization of linear polymers with chain folding. In: Hannay NB, editor. Treatise on solid state chemistry, vol. 3. New York: Plenum; 1976. p. 497–614 [chapter 7].
[62] Frank FC, Tosi M. Proc R Soc (London) 1961;A263:323.
[63] Hoffman JD. Polymer 1982;23:656.
[64] Frank FC. J Cryst Growth 1974;22:233.
[65] Sanchez IC, DiMarzio EA. J Res Natl Bur Stand 1972;76A:213.
[66] Hoffman JD, Guttman CM, DiMarzio EA. Disc Faraday Soc 1979; 68:177.
[67] Mansfield ML. Polymer 1988;29:1755.
[68] Toda A. Polymer 1991;32:771.
[69] Passaglia E, Khoury F. Polymer 1984;25:631.
[70] Hoffman JD. Polymer 1983;24:3.
[71] Hoffman JD, Miller R. Polymer 1997;38:3151.

[72] Point JJ. Disc Faraday Soc 1979;68:167.
[73] Point JJ. Macromolecules 1979;12:770.
[74] Phillips PJ. Rep Prog Phys 1990;53:549.
[75] Phillips PJ. Mater Sci Technol 2003;19:1153.
[76] Hoffman JD, Miller RL. Macromolecules 1989;22:3502.
[77] Laruritzen Jr JI, Passaglia E. J Res Natl Bur Stand 1967;71A:261.
[78] Hoffman JD, Lauritzen Jr JI, Passaglia E, Ross GS, Frolen LJ, Weeks JJ. Kollod Z Z Polym 1969;231:564.
[79] Point JJ, Colet MC, Dosière M. J Polym Sci, Polym Phys Ed 1986; 24:357.
[80] Hoffman JD. Polymer 1985;26:803.
[81] Hoffman JD. Polymer 1985;26:1763.
[82] Ungar G, Keller A. Polymer 1986;27:1835.
[83] Hoffman JD. Polymer 1991;(32):2828.
[84] Hoffman JD. Polymer 1992;33:2643.
[85] Hoffman JD, Miller RL, Marand H, Roitman DB. Macromolecules 1992;25:2221.
[86] Hoffman JD, Miller RL. Macromolecules 1989;22:3038.
[87] Miller RL, Hoffman JD. Polymer 1991;32:963.
[88] Armistead JP, Hoffman JD. Macromolecules 2002;35:3895.
[89] Cheng SZD, Lotz B. Philos Trans R Soc London A 2003;361:517.
[90] Ergoz E, Fatou JG, Mandelkern L. Macromolecules 1972;5:147.
[91] Pelzbauer Z, Galeski A. J Polym Sci Part C 1972;38:23.
[92] Alamo R, Fatou JG, Guzman J. Polymer 1982;23:379.
[93] Barham PJ, Jarvis DA, Keller A. J Polym Sci, Polym Phys Ed 1982; 20:1733.
[94] Vasanthakumari R, Pennings AJ. Polymer 1983;24:175.
[95] Barham PJ, Keller A, Oltun EL, Holmes PA. J Mater Sci 1984;19: 2781.
[96] Clark EJ, Hoffman JD. Macromolecules 1984;17:878.
[97] Lovinger AJ, Davis DD, Padden Jr FJ. Polymer 1985;26:1595.
[98] Organ SJ, Keller A. J Polym Sci, Polym Phys Ed 1986;24:2319.
[99] Allen RC, Mandelken L. Polym Bull 1987;17:473.
[100] Phillips JP, Vantansever N. Macromolecules 1987;20:2138.
[101] Lazcano S, Fatou JG, Marco C, Bello A. Polymer 1988;29:2076.
[102] Roitman DB, Marand H, Miller RL, Hoffman JD. J Phys Chem 1989; 93:6919.
[103] Cheng SZD, Janimak JJ, Zhang A, Cheng HN. Macromolecules 1990;23:298.
[104] Cheng SZD, Chen JH, Janimak JJ. Polymer 1990;31:1018.
[105] Lambert WS, Phillips PJ. Macromolecules 1994;27:3537.
[106] Rodriguez-Arnold J, Bu Z, Cheng SZD, Hsieh ET, Johnson TW, Geerts RG, et al. Polymer 1994;35:5194.
[107] Lambert WS, Phillips PJ. Polymer 1996;37:3585.
[108] Wagner J, Phillips PJ. Polymer 2001;42:8999.
[109] Abe H, Kikkawa Y, Inoue Y, Doi Y. Biomacromolecules 2001;2: 1007.
[110] Kovacs AJ, Gonthier A. Kolloid-Z u Z Polym 1972;250:530.
[111] Kovacs AJ, Gonthier A, Straupe C. J Polym Sci, Polym Symp 1975; 50:283.
[112] Kovacs AJ, Straupe C, Gonthier A. J Polym Sci, Polym Symp 1977; 59:31.
[113] Kovacs AJ, Straupe C. Disc Faraday Chem Soc 1979;68:225.
[114] Kovacs AJ, Straupe C. J Cryst Growth 1980;48:210.
[115] Cheng SZD, Chen JH. J Polym Sci, Polym Phys Ed 1991;29:311.
[116] See an early review, Wunderlich B. Macromolecular physics. Crystal, morphology, defects, vol. 1. New York: Academic Press; 1973 [chapter 3].
[117] Leung WM, Manley RS, Panaras AR. Macromolecules 1985;18:760.
[118] Cheng SZD, Chen JH, Heberer DP. Polymer 1992;33:1429.
[119] Hoffmand JD. Macromolecules 1985;18:772.
[120] Lindenmeyer PH, Holland VF. J Appl Phys 1964;35:55.
[121] Magill JH. J Appl Phys 1964;35:3249.
[122] Magill JH. J Polym Sci Part A-2 1967;5:89.
[123] Magill JH. J Polym Sci Part A-2 1969;7:1187.
[124] van Antwerpen F, van Krevelen DW. J Polym Sci, Polym Phys Ed 1972;10:2423.
[125] Lovering EF. J Polym Sci Part C 1970;30:329.
[126] Garza J, Marco C, Fator JG, Bello A. Polymer 1981;22:377.
[127] Pérez E, Bello A, Fatou JG. Colloid Polym Sci 1984;262:605.
[128] Cheng SZD, Wudenrlich B. J Polym Sci, Polym Phys Ed 1986;24: 595.
[129] Hoffman JD, Miller RL. Macromolecules 1988;21:3038.
[130] Cheng SZD, Wunderlich B. J Polym Sci, Polym Phys Ed 1986;24: 577.
[131] Cheng SZD, Bu H, Wunderlich B. J Polym Sci, Polym Phys Ed 1988;26:1947.
[132] Geil PH. Polymer 2000;41:8983.
[133] Wunderlich B. Disc Faraday Chem Soc 1979;68:239.
[134] Hikosaka M. Polymer 1987;28:1257.
[135] Hikosaka M. Polymer 1990;31:458.
[136] Sadler DM. Polym Commun 1986;27:140.
[137] Sadler DM. Nature 1987;326:174.
[138] Sadler DM, Gilmer GH. Phys Rev Lett 1986;56:2708.
[139] Sadler DM. J Chem Phys 1987;87:1771.
[140] Sadler DM. Polymer 1987;28:1140.
[141] Sadler DM. Polym Commun 1987;28:242.
[142] Sadler DM, Gilmer GH. Phys Rev B 1988;38:5684.
[143] Armitstead K, Goldbeck-Wood G. Adv Polym Sci 1992;100:221.
[144] Flory PJ. Trans Faraday Soc 1955;51:848.
[145] Sanchez IC, Eby RK. Macromolecules 1973;6:631.
[146] Sanchez IC. J Polym Sci, Polym Symp 1977;59:109.
[147] See for example, Wunderlich B. Macromolecular physics. Crystal melting, vol. 3. New York: Academic Press; 1980.
[148] Fu Q, Chiu FC, McCreight KW, Guo MM, Tseng WW, Cheng SZD, et al. J Macromol Sci Phys 1997;B36:41.
[149] Alizadeh A, Richardson L, Xu J, McCartney S, Marand H, Cheung YW, et al. Macromolecules 1999;32:6221.
[150] Chiu FC, Wang Q, Fu Q, Honigfort P, Cheng SZD, Hsiao BS, et al. J Macromol Sci Phys 2000;B39:317.
[151] Alamo RG, Blanco JA, Agarwal PK, Randall JC. Macromolecules 2003;36:1559.
[152] Hosier IL, Alamo RG, Esteso P, Isasi JR, Mandelkern L. Macromolecules 2003;36:5623.
[153] Dai PS, Cebe P, Capel M, Alamo RG, Mandelkern L. Macromolecules 2003;36:4042.
[154] Hosier IL, Alamo RG, Lin JS. Polymer 2004;(45):3441.
[155] Cheng SZD, Janimak JJ, Zhang A, Hsien ET. Polymer 1991;32:648.
[156] Janimak JJ, Cheng SZD, Giusti PA, Hsieh ET. Macromolecules 1991;24:2253.
[157] Janimak JJ, Cheng SZD, Zhang A. Polymer 1992;33:728.
[158] Flory PJ. Statistical mechanics of chain molecules. New York: Interscience; 1969.
[159] Turner-Jones A, Aizlewood JM, Beckett DR. Makromol Chem 1964; 75:134.
[160] Hikosaka M, Seto T. Polym J 1973;5:111.
[161] Petraccone V, De Rosa C, Guerra G, Tuzi A. Makromol Chem Rapid Commun 1984;5:631.
[162] Guerra G, Petraccone V, Corradini P. Eur Polym J 1984;29:937.
[163] Petraccone V, Guerra G, De Rosa C, Tuzi A. Macromolecules 1985; 18:813.
[164] Napolitano R, Pirozzi B, Varriale V. J Polym Sci, Polym Phys Ed 1990;28:138.
[165] Auriemma F, Ruiz de Ballesteros O, De Rosa C, Corradini P. Macromolecules 2000;33:8764.
[166] Lotz B, Graff S, Straupe C, Wittmann JC. Polymer 1991;32:2902.
[167] Lotz B. Eur Phys J E 2000;3:185.
[168] Lotz B. Adv Polym Sci, in press.
[169] Natta G, Corradini P, Ganis P. Nuovo Cimento Suppl 1960;15:83.
[170] Natta G, Peraldo M, Corradini P. Rend Acad Naz Lincei 1959;24:14.
[171] Miller RL. Polymer 1960;1:135.
[172] Atkins EDT, Isaac DH, Keller A. J Polym Sci, Polym Phys Ed 1980; 18:71.
[173] Keller A. Disc Faraday Soc 1995;101:1.

[174] Brückner S, Allegra G, Corradini P. Macromolecules 2002;35:3928.
[175] Aleman C, Lotz B, Puiggali J. Macromolecules 2001;34:4795.
[176] Sasaki S, Asakura T. Macromolecules 2003;36:8385.
[177] Cartier L, Okihara T, Lotz B. Macromolecules 1997;30:6313.
[178] See for example, Organization of macromolecules in the condensed phase. Disc Faraday Soc 1979.
[179] Arlie JP, Spegt PA, Skoulios AE. Makromol Chem 1966;99:160.
[180] Arlie JP, Spegt PA, Skoulios AE. Makromol Chem 1967;104:212.
[181] Spegt P. Makromol Chem 1967;139:139.
[182] Ungar G, Stejny J, Keller A, Bidd I, Whiting MC. Science 1985;229: 386.
[183] Ungar G, Keller A. Polymer 1987;28:1899.
[184] Cheng SZD, Zhang AQ, Chen JH, Heberer DP. J Polym Sci, Polym Phys Ed 1991;29:287.
[185] Cheng SZD, Chen JH, Zhang AQ, Heberer DP. J Polym Sci, Polym Phys Ed 1991;29:299.
[186] Cheng SZD, Zhang A, Barley JS, Chen JH, Habenschuss A, Zschack PR. Macromolecules 1991;24:3937.
[187] Cheng SZD, Chen JH, Zhang AQ, Barley JS, Habenschuss A, Zschack PR. Polymer 1992;33:1140.
[188] Cheng SZD, Chen JH, Barley JS, Zhang AQ, Habenschuss A, Zschack PR. Macromolecules 1992;25:1453.
[189] Cheng SZD, Wu SS, Chen JH, Zhuo Q, Quirk RP, von Meerwall ED, et al. Macromolecules 1993;26:5105.
[190] Lee SW, Chen EQ, Zhang AQ, Yoon Y, Moon BS, Lee S, et al. Macromolecules 1996;29:8816.
[191] Chen EQ, Lee SW, Zhang A, Moon BS, Honigfort PS, Mann I, et al. Polymer 1999;40:4543.
[192] Organ SJ, Ungar G, Keller A. Macromolecules 1989;22:1995.
[193] Organ SJ, Barham PJ, Hill MJ, Keller A, Morgan RL. J Polym Sci, Polym Phys Ed 1997;35:1775.
[194] Boda E, Ungar G, Brooke GM, Burnett S, Mohammed S, Proctor D, et al. Macromolecules 1997;30:4647.
[195] Sutton SJ, Vaughan AS, Bassett DC. Polymer 1996;37:5735.
[196] Morgan RL, Barham PJ, Hill MJ, Keller A, Organ SJ. J Macromol Sci Phys 1998;B37:319.
[197] Hobbs JK, Hill MJ, Barham PJ. Polymer 2001;42:2167.
[198] Ungar G, Mandal P, Higgs PG, de Silva DSM, Boda E, Chen CM. Phys Rev Lett 2000;85:4387.
[199] Hosier IL, Bassett DC, Vaughan AS. Macromolecules 2000;33: 8781.
[200] Hosier IL, Bassett DC, Vaughan AS. Macromolecules 2000;33: 8781.
[201] Ungar G, Zeng X. Chem Rev 2001;101:4157.
[202] Wunderlich B, Metha A. J Polym Sci, Polym Phys Ed 1974;12:255.
[203] Sadler DM. J Polym Sci, Polym Phys Ed 1971;9:779.
[204] Tsuji H, Ikada Y. Macromolecules 1993;26:6918.
[205] Tsuji H, Ikada Y. Polymer 1999;40:6699.
[206] Alfonso GC, Russell TP. Macromolecules 1986;19:1143.
[207] Di Lorenzo ML. Prog Polym Sci 2003;28:663.
[208] Mareau VH, Prud'homme RE. Macromolecules 2003;36:675.
[209] Chen WY, Li CY, Zheng JX, Huang P, Zhu L, Ge Q, et al. Macromolecules 2004;37:5292.
[210] Frank FC. Disc Faraday Soc 1949;5:186.
[211] Stranski I. Disc Faraday Soc 1949;5:69.
[212] Dawson IM. Proc R Soc (London) 1952;A214:72.
[213] Khoury F. J Appl Phys 1963;34:73.
[214] Khoury F, Padden Jr FJ. J Polym Sci 1960;18:455.
[215] Bassett DC, Keller A. Philos Mag 1962;7:81.
[216] Sadler DM, Barber M, Lark G, Hill MJ. Polymer 1986;27:25.
[217] Loo YL, Register RA, Ryan AJ. Phys Rev Lett 2000;84:4120.
[218] Huang P, Zhu L, Calhoun BH, Ge Q, Quirk RP, Cheng SZD, et al. Macromolecules 2001;34:6649.
[219] Zhu L, Cheng SZD, Calhoun BH, Ge Q, Quirk RP, Thomas EL, et al. J Am Chem Soc 2000;122:5957.
[220] Zhu L, Huang P, Chen WY, Ge Q, Quirk RP, Thomas EL, et al. Macromolecules 2002;35:3553.
[221] Zhu L, Chen Y, Zhang AQ, Calhoun BH, Chun MS, Quirk RP, et al. Phys Rev B 1999;60:10022.
[222] Zhu L, Mimnaugh BR, Ge Q, Quirk RP, Cheng SZD, Thomas EL, et al. Polymer 2001;42:9121.
[223] Xu JT, Fairclough JPA, Mai SM, Ryan AJ, Chaibundit C. Macromolecules 2002;35:6937.
[224] Xu JT, Fairclough JPA, Mai SM, Chaibundit C, Mingvanish M, Booth C, et al. Polymer 2003;44:6843.
[225] Xu JT, Fairclough JPA, Mai SM, Ryan AJ. J Mater Chem 2003;13: 2740.
[226] Huang P, Zhu L, Guo Y, Ge Q, Jing AJ, Chen WY, et al. Macromolecules 2004;37:3689.
[227] Chen WY, Zheng JX, Cheng SZD, Li CY, Huang P, Zhu L, et al. Phys Rev Lett 2004;93:028301.
[228] Lee LBW, Register R. Macromolecules 2004;37:7278.
[229] DiMarzio EA, Guttman CM, Hoffman JD. Macromolecules 1980;13: 1194.
[230] Ungar G, Feijoo JL, Keller A, Yord R, Percec V. Macromolecules 1990;23:3411.
[231] Percec V, Keller A. Macromolecules 1990;23:4347.
[232] Cheng SZD, Yandrasits MA, Percec V. Polymer 1991;32:1284.
[233] Yandrasits MA, Cheng SZD, Zhang A, Cheng J, Wunderlich B, Percec V. Macromolecules 1992;25:2112.
[234] Jing AJ, Taikum O, Li CY, Harris FW, Cheng SZD. Polymer 2002; 43:3431.
[235] Pardey R, Zhang A, Gabori PA, Harris FW, Cheng SZD, Adduci J, et al. Macromolecules 1992;25:5060.
[236] Pardey R, Shen DX, Gabori PA, Harris FW, Cheng SZD, Adduci J, et al. Macromolecules 1993;26:3687.
[237] Pardey R, Wu SS, Chen JH, Harris FW, Cheng SZD, Keller A, et al. Macromolecules 1994;27:5794.
[238] Keller A, Cheng SZD. Polymer 1998;39:4461.
[239] Harrowell PR, Oxtoby DW. J Chem Phys 1984;80:1639.
[240] Kelton KF. In: Ehrenreich H, Turnbull D, editors. Solid state physics, vol. 45. New York: Academic; 1991. p. 75.
[241] Debebedetti PG. Metastable liquids. New Jersey: Princeton University; 1996.
[242] Cheng SZD, Keller A. Ann Mater Sci 1998;28:533.
[243] Olmsted PD, Poon WCK, McLeish TCB, Terrill NJ, Ryan AJ. Phys Rev Lett 1998;81:373.
[244] Imai M, Kaji K, Kanaya T. Phys Rev Lett 1993;71:4162.
[245] Matsuba G, Kanaya T, Saito M, Kaji K, Nishida K. Phys Rev E 2000; 62:R1497.
[246] Liu L, Muthukumar M. J Chem Phys 1998;109:2536.
[247] Muthukumar M. Philos Trans R Soc London A 2003;361:538.
[248] Vonnegut B. J Colloid Sci 1948;3:563.
[249] Massa MV, Carvalho JL, Dalnoki-Veress K. Eur Phys J E 2003;12: 111.
[250] Massa MV, Dalnoki-Veress K. Phys Rev Lett 2004;92:255509.
[251] Lotz B, unpublished experimental data obtained by Professor A.J. Kovacs.
[252] Strobl G. Eur Phys J E 2000;3:165.
[253] Cheng SZD, Li CY, Zhu L. Eur Phys J E 2000;3:195.
[254] Muthukumar M. Eur Phys J E 2000;3:199.
[255] Adamovsky S, Schick C. Thermochim Acta 2004;415:1 [and private conversations].